WESTERN AUSTRALIAN Impact Craters

Field Excursion

20-29 August 2012

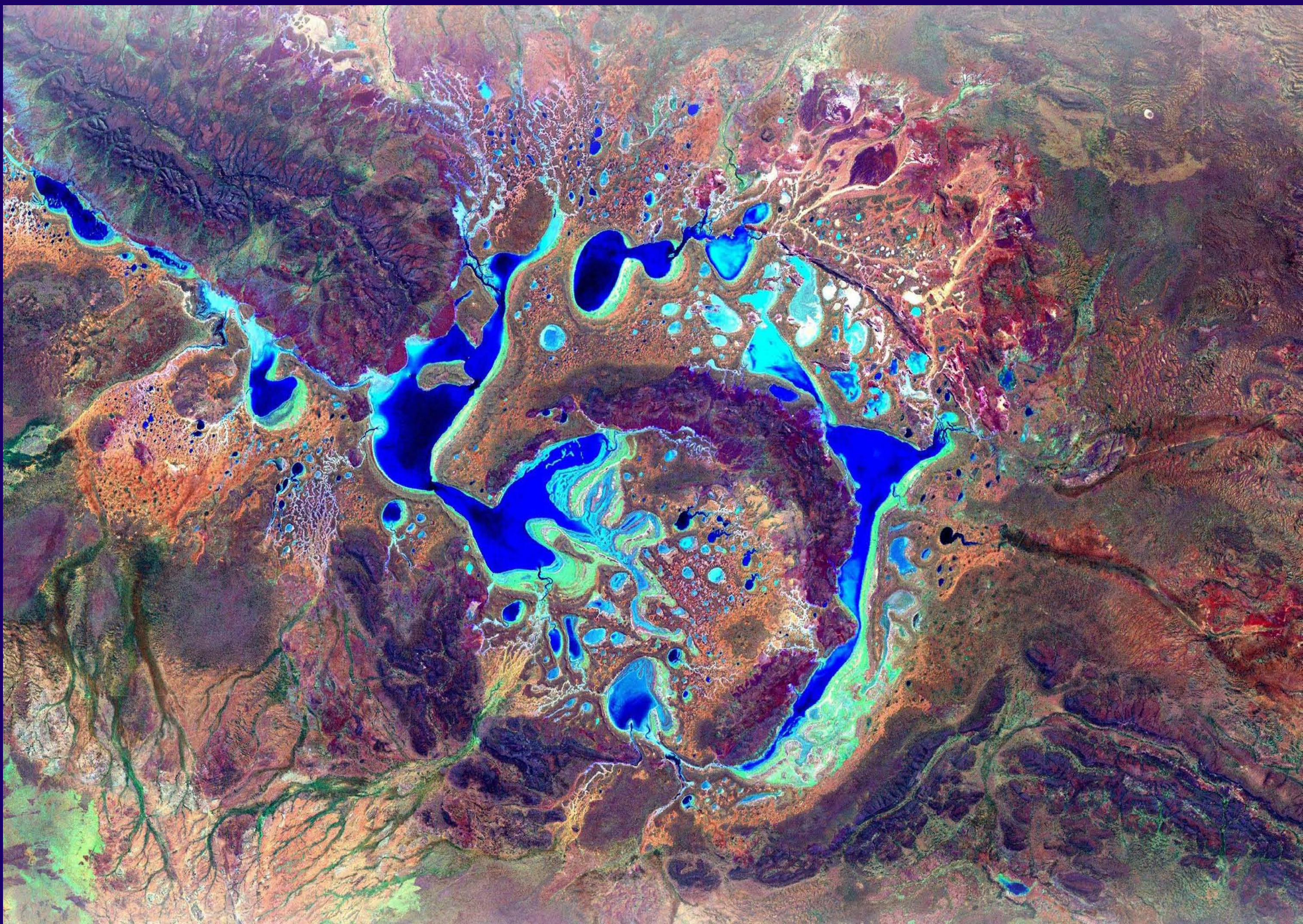

75th Annual Meeting of the Meteoritical Society

12-17 August 2012

Cairns Australia

This field guide was compiled and edited by Jenny Bevan (August 2012).

The corresponding author for enquiries is Dr Alex Bevan; postal address: Western Australian Museum, Locked Bag 49, Welshpool DC, WA 6986, or email: Alex.Bevan@museum.wa.gov.au.

Front Cover: Detail of Landsat Enhanced Thematic Mapper satellite image of the Shoemake Impact Structure, 100 km NE of Wiluna, WA, acquired 5 May 2000. False colour image enhancement by assigning red pixels to infrared light (Band 7), green pixels to near infrared light (Band 4), and blue pixels to visible blue light (Band 1).

The image has been further enhanced by merging the colour information with a high resolution B&W image of the same area to produce an apparent pixel resolution of 14.25 m. Blue and cyan areas signify ephemeral salt lakes, green signifies vegetation, pale brown signifies bare soil, and the various shades of dark reddish brown signify exposed rock. North is up; horizontal field of view is about 50 km.

Data courtesy of Global Land Cover Facility, University of Maryland.

The Western Australian Impact Craters Field Excursion

(Post Meteoritical Society Conference Excursion)
Monday 20 Aug 2012 to Wednesday 29 Aug 2012

Leaders: Alex Bevan, John Bunting and Mike Freeman

SPONSORS

Atlas Iron
Australian Government: Department of Industry, Innovation Science, Research and Tertiary Education
Australian National University
Australian Scientific Instruments
Barringer Crater Company
Cameca
Government of Western Australia: Department of Mines and Petroleum
Geological Survey of Western Australia
International Meteorite Collectors Association
Japan Aerospace Exploration Agency
Lunar and Planetary Institute
The Meteoritical Society
National Aeronautics and Space Administration
Planetary Studies Foundation
ThermoFisher Scientific
Wiley Publishing
Western Australian Museum

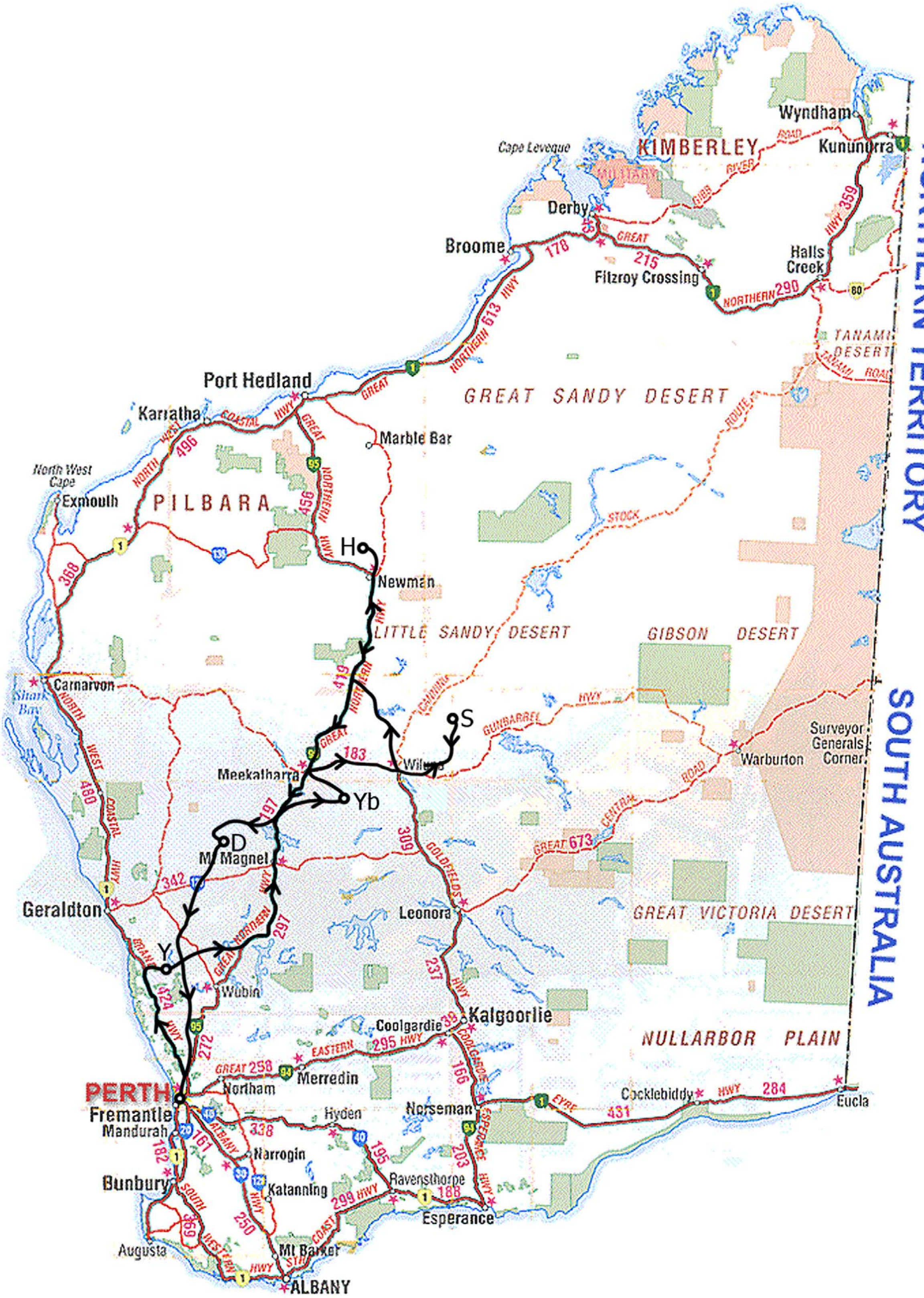

Figure 1: Map of the route, showing sites visited. These are (in order) Y: Yallalie Impact Structure; Yb: Yarrabubba Impact Structure; S: Shoemaker Impact Structure; H: Hickman Crater; D: Dalgaranga Crater. Base map taken from aptouring.com.au website.

Program and route

DAY 1. Monday 20th August

From Perth heading north to the **Yallalie Impact Structure** we will travel within the Perth Basin for around 200 km along a route which runs parallel to first the Darling Scarp and then the Gingin Scarp. Changes in vegetation match the varying lithologies. The drive is mostly on Cenozoic sand and limesand (locally cemented marine to eolian limestone) with interdune swales containing lakes, before we reach the Dandaragan Trough and Cretaceous rocks. A further 20km or so brings us to the first stop.

From Yalallie we head east, crossing the Neoproterozoic Moora Group located east of the Darling Fault, and then over the Archean granites and metasediments of the Southwest Terrane of the Yilgarn Craton to Dalwallinu, our stop for the first night, located about 85 km east-northeast of Yalallie.

Distance travelled: 370 km.

DAY 2. Tuesday 21st August

We follow the Great Northern Highway, crossing the Yilgarn Craton. The first 60 km are through wheatbelt farmland, but then we enter the uncleared “outback” where mining and cattle or sheep grazing are the prime land uses. Then after another 70 km we pass the new iron ore mining development of Mt Gibson. After passing through Paynes Find, Mount Magnet and Cue, gold-mining towns that have past their heydays, we turn off the highway and head east to Yarrabubba. Total distance for the day is nearly 500 km. We spend the night camping within the **Yarrabubba Impact Structure.**

Distance travelled: 365km.

DAY 3. Wednesday 22nd August

The day will be spent examining aspects of the **Yarrabubba Impact Structure** and again we will camp overnight in the structure.

Distance travelled: local.

DAY 4. Thursday 23rd August

Leaving Yarrabubba, we drive 80 km to Meekatharra, then turn east, passing the former gold-mining town of Wiluna after another 180 km, and then on 80 km to Millrose Homestead from where we “head bush” for 60 km northward along station tracks to the **Shoemaker Impact Structure**. As we approach the end of the day the topography changes as we cross into the sedimentary Earaheedy Basin rocks. Ironstones of the Frere Formation form a conspicuous, though low, ridge. Overnight is a bush camp.

Distance travelled: 450km.

DAY 5. Friday 24th August

Today is spent examining aspects of the **Shoemaker Impact Structure** followed by another bush camp.

Distance travelled: local.

DAY 6. Saturday 25th August

We leave the **Shoemaker Impact Structure** after a last look, for the **Hickman Meteorite Crater.** Returning through to Wiluna, we then follow a main road to the northwest to the Great Northern Highway, about 180 km past the town. From about 90 km past Wiluna we leave the Yilgarn Craton and start driving over the sediments of the Bryah and Yerrida basins, components of the Capricorn Orogen. After about 70 km on the sediments we then cross on to the Marymia Inlier, which is part of the granite-greenstone terrane of the Yilgarn Craton.

About 90 km along the Great Northern Highway we arrive at Kumarina, a tavern and petrol stop, that is our overnight stay. The last 70 km part of the route crosses the Collier Basin sediments of the Capricorn Orogen.

Distance travelled: 490km.

DAY 7. Sunday 26th August

Leaving Kumarina we continue northwards across Collier Basin sediments for 95 km, and then over the granite-greenstones of the Sylvania Inlier, part of the crystalline basement of the Pilbara Craton. We pass the iron ore mining town of Newman after 150 km. The Ophthalmia Range is on the north of the town and behind Newman is the Mount Whaleback iron ore open cut, while to the east of the highway are the Mount Newman open cuts, all operated by BHP-Billiton. We continue along the Marble Bar road until we leave it to follow BHP-B's iron ore railway line for about 10 km before heading bush for another 35 km along very slow and rough tracks to the **Hickman Crater**. After examining the crater we will camp for the night at the nearby Atlas Iron Ore exploration camp.

Distance travelled: 255km.

DAY 8. Monday 27th August

If time permits we will have a further opportunity to look at the **Hickman Crater** before returning to the Great Northern Highway and heading south towards Meekatharra. We will camp before reaching the town after a drive of some 500 km.

Distance travelled: 500km.

DAY 9. Tuesday 28th August

We drive from Meekatharra to Cue, a distance of about 170 km, then head west for another 95 km to the **Dalgaranga Crater** for a look at this 25 m feature excavated in the Yilgarn Craton weathered granite. We then leave Dalgaranga, heading southwest to Yalgoo and then on to Morawa for overnight at Morawa Hotel, about 240 km from the crater.

Distance travelled: 500km.

DAY 10. Wednesday 29th August

We leave Morawa and continue for about 350 km to Perth. The road passes the township of Moora, the source of the Moora Group. North of the town we pass the Moora chert quarries where totally silicified stromatolitic Proterozoic carbonate rocks are mined and used for silicon manufacture in a plant located 180 km south of Perth. Along this section we are travelling in close proximity to the Darling Fault, the western margin of the Yilgarn Craton. Return to accommodation in Perth.

Distance travelled: 380km. Total distance covered for the excursion is about 3500 km.

Please be aware that you take part in the excursion at your own risk.

As well as complying with the instructions given by the tour leaders, the following general safety precautions should be followed:

1. Keep within sight of other excursion participants at all times while we are at fieldsites. Do not wander off on your own.

2. Wear a broad-brim hat and full-length loose-fitting light clothes to guard against the effects of the intense sun. In particular make sure your feet, legs and arms are adequately protected from sunburn.

3. On a regular basis apply sun protection lotion (preferably 30+ rating) to exposed parts of your body.

4. Keep drinking water (at least 2 litres per day). Dehydration and heat stroke are real dangers and can simply be avoided by drinking water.

5. When walking in the bush, look out for snakes. Do not approach snakes. Make noise as you walk - this usually frightens these reptiles.

6. When wading in water wear protective footwear.

7. The bush flies are harmless, although a nuisance while eating outside. A way to overcome this problem is to wet your back - a cloud of flies will settle there and hopefully stay away from your face. Mosquitoes and sand flies may be a problem at some sites and you should apply insect repellent.

8. If you smoke, do not discard cigarette butts in the bush. These are major fire hazards. Smoking is not permitted in restaurants, shops, clubs or buses in Western Australia, and certainly not in our vehicles.

Regional geology

Mike Freeman

The area visited in the course of the excursion is dominated by two Archean cratons (Yilgarn and Pilbara), and an intervening Neoarchean-Neoproterozoic complex plate-plate collision zone (Capricorn Orogen). The two orogens are surrounded and onlapped by Palaeozoic sedimentary basins and the whole has been subjected to prolonged arid weathering that has generated a thick and complex regolith. Figure 3 overleaf shows the overall geology of the State with the locations of the proven extraterrestrial impact structures.

Impacts of extraterrestrial objects have punctuated these rocks and sediments, and there is evidence of thirteen confirmed impacts, of which this excursion will examine five. From oldest to youngest they are: the **Yarrabubba Structure** in the Archean Yilgarn Craton, the **Shoemaker Impact Structure** in the edge of the Earaheedy Basin that also involved the Yilgarn Craton, the **Yalallie Impact Structure** that affected the Mesozoic Perth Basin while the sediments were still accumulating, **Hickman Crater** in the Archean Hamersley Basin sediments and **Dalgaranga Crater** that occurs in granites of the Yilgarn Craton.

Yilgarn Craton

The Yilgarn Craton covers an area of 657 000 km^2 in the southwestern part of Australia and consists of granite, granitic gneiss and linear to ovoid greenstone belts trending roughly north-south. The rocks are of Archean age, ranging from 3850 Ma to 2500 Ma. However in places they contain rare zircon grains dated up to 4410 Ma in the Jack Hills (Wilde et al., 2001) or 4350 Ma in the Southern Cross region (Wyche et al., 2004), which are the oldest terrestrial material known on Earth. The craton extends some 1000 km north-south and 600 km east-west.

Figure 2: 'Greenstone belts' near Paynes Find show typical expression as elongate, dark hills covered with vegetation, in comparison with the granites which tend to weather topographically lower and are generally less well-vegetated.

Granites comprise about half of the craton and are the most common rock type and granitic gneiss (almost solely orthogneiss), while less common, is dominant in the southwest and northwest parts of the craton. 'Greenstone belts' are metamorphosed packages of volcanic and sedimentary rocks that have been slightly to severely deformed. The volcanics include basalts, rhyolite, andesite and komatiite. The eruptive environment is commonly shallow marine and pillow basalts and water-lain volcanigenic sediments are common. There are also sills and other minor intrusives. Sedimentary rocks include conglomerate, sandstone, black shales, chert and banded iron formation.

The Yilgarn Craton is bounded to the west by the Darling Fault, a long-lived structure that extends for at least 1000 km from the south coast to east of Shark Bay (Figure 3 overleaf). To the north the Yilgarn Craton merges into a zone of younger sediments and metamorphic rocks, referred to as the Capricorn Orogen, that constitute a collision zone between the Yilgarn Craton and the Pilbara Craton. To the south the Yilgarn Craton abuts the Mesoproterozoic Albany-

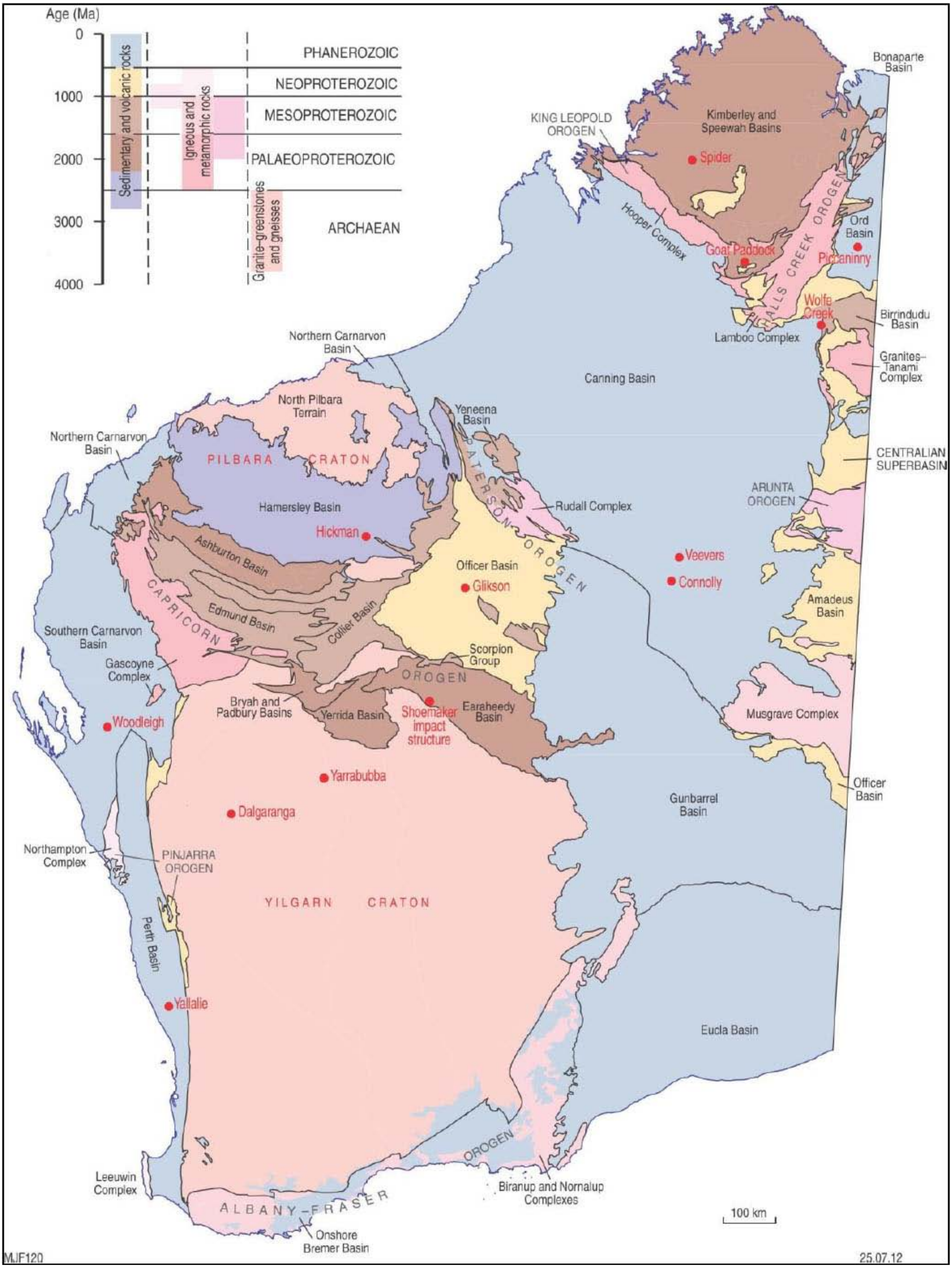

Figure 3: Western Australia, showing the main geological elements and impact structures (with permission of the Geological Survey of Western Australia).

Fraser Orogen that represents the sutured collision zone between itself and the Gawler Craton, while to the east it is progressively overlapped by ever-thicker Palaeozoic sedimentary rocks of the Gunbarrel Basin.

Large changes in our understanding of the greenstone belts have been made in recent years through ever-more-detailed mapping by the Geological Survey in collaboration with Geoscience Australia and various universities. Of particular importance has been the use of more detailed sampling and geochronology using SHRIMP (Super High Resolution Ion Microprobe) dating of detrital, metamorphic and igneous zircons.

Cratons are divided into terranes, which are unified blocks of basement rocks that commonly are fault-bounded and have an internally consistent geological history which differs from that of adjacent terranes.On the excursion we cross firstly the Southwest Terrane, then the Youanmi Terrane after we leave the farming region and, as we approach the Shoemaker Impact Structure, the Eastern Goldfields Terrane. Then we will cross the Marymia Inlier northwest of the Shoemaker Impact Structure, surrounded by sediments of the Capricorn Orogen. This 200 km x 100 km inlier of granite-greenstone has become important economically since the mid-1990s as containing a number of important gold deposits.

Most of the Yilgarn Craton's greenstone belts host gold deposits, with the Golden Mile at Kalgoorlie being the largest, having produced some 2140 t of gold since its discovery in 1893. Unusual komatiites, with Mg contents of over 13%, host major nickel sulphide deposits (e.g. Kambalda, Mount Keith) that supply some 20% of the world's nickel metal. At Golden Grove, about 50 km northwest of Mt Gibson (passed on the excursion), felsic volcanics host large deposits of lead-zinc-silver-copper metals as massive to disseminated sulphides in volcanic piles.

Pilbara Craton

The Pilbara Craton is the northern of the two western Archean cratons in Western Australia. The Pilbara has an area of 200 000 km^2 extending 450 km east-west and 300 km north-south. The northern 60 000 km^2 consists of granite-greenstone terranes and the southern 140 000 km^2 is dominated by Archean sediments and volcanics (the Hamersley Basin). On the southeastern margin of the craton is an inlier of the granite-greenstones terrane referred to as the Sylvania Inlier, which the excursion route crosses as it approaches the iron-ore-mining town of Newman.

The granite-greenstone terrane contains a number of conspicuous near-circular domes of granite that are surrounded by steeply-dipping sedimentary-volcanic sequences, commonly in the form of synclines. This distribution of the rock distribution and arrangement is related by some researchers to be pre-plate-tectonic orogenesis (Hickman, 2012) dating from about 3.0 Ga.

The Pilbara Craton is very significant geologically for the excellently-preserved stratigraphy and structural geology (potentially from pre-plate tectonic times) and for the evidence of early life that it contains, though there is still some debate about some of the fossils or pseudofossils. Of major importance is that the 3.48 Ga Dresser Formation contains stromatolites, microfossils and putative organic carbon (Hickman, 2012) at localities about 250 km north of the town of Newman that we pass through. These are amongst the very oldest fossils on Earth and are being studied by, for example, NASA as proxies for identifying possible Martian landing sites to give the best probability of targeting sites where life may have lived on that planet.

Hamersley Basin of the Pilbara Craton

Hamersley Basin sediments overlie the southern parts of the Pilbara Craton, consisting of a lower Fortescue Group and an upper Hamersley Group. The Fortescue Group, with a thickness of some 3.7 km, includes mudstone, siltstone, shale and minor conglomerate and dolostone of Neoarchean age. Overlying this is the Hamersley Group of eight formations measuring some 1.8 km in thickness, dominated by banded iron-formation ('BIF') that has world-ranking economic importance, and is of latest Archean to Paleoproterozoic age. The

Figure 4: Banded iron formation (BIF).

Hickman meteorite struck near the contact of the uppermost BIF-bearing unit, the Boolgeeda Iron Formation, and the underlying Woongarra Rhyolite, a 300m-thick rhyolite to rhyodacite unit, with BIF horizons and jaspilite units within the centre parts (Tyler, 1994).

Within the Fortescue and Hamersley Groups there are three main iron formations: Marra Mamba; Brockman and Boolgeeda that host the majority of the iron ore of the Pilbara (Trendall and Blockley, 1970). In addition to other resources in the Pilbara (such as secondary iron ore and of deposits in river channels), total resources stand at 35 000 Gt, but with some very large upsides if beneficiation of the ore is economically possible in the future. Newman, on our route, is an iron ore town established by BHP-Billiton in the 1960s and sends iron ore by a dedicated railway 425 km to Port Hedland.

Capricorn Orogen

A number of stratigraphic and structural units and up to seven deformation events represent the collision and post-collision sedimentation through the impact and suturing of the Yilgarn and Pilbara Cratons (and including the Glengburgh Terrane) between 2.15 and 1.07 Ga.

The Palaeoproterozoic to Mesoproterozoic Bryah, Padbury, Yerrida, Edmund, Collier and Earaheedy Basins at the present day cover a total area of ca 175 000 km^2 and are distributed throughout the orogen except in the southwest corner where the Glengburgh Terrane occurs. This Terrane is now thought to be a separate pre-collision area of early crystalline basement (Johnson et al., 2011). These basins form part of the Capricorn Orogen and can be considered as later-phase accumulations across the orogen derived from tectonism within and external to the orogen. Recent mapping and geochronology by the Geological Survey of WA and other organisations have led to redefinitions of units and their relationships. For example, the Bryah, Padbury and Yerrida Basins, were formerly considered as one geological entity, the Glengarry Basin but are recognised to be characterized by distinct stratigraphy, igneous activity, structural and metamorphic history, and mineral deposit types. The Bryah and Yerrida Basins contain voluminous eruptive tholeiitic volcanics. In the Bryah Basin tholeiitic volcanic rocks are Mg-rich and have mixed MORB to oceanic island chemical signatures, but with a boninitic (subduction-related) component. In the Yerrida Basin tholeiites are Fe-rich and have chemical signatures that suggest a mixed tectonic environment ranging from oceanic to continental. Considering such evidence is still allowing revision of the geology of the orogen.

Of significance for the excursion is that the route crosses some 200 km of the Collier Basin sediments. These consist of up to 4 km of siliciclastic and carbonate sediments that were deposited after the Mutherbukin Tectonic Event dated at at 1.38 Ga, before dolerite intrusions at 1.07 Ga (Thorne et al., 2011).

The Earaheedy Basin contains a sequence of shale, siltstone, sandstone, iron-formation and stromatolitic carbonate rocks. It is up to 5000 m thick, overlaps the northeastern edge of the Yilgarn Craton and is unconformable on the old Yilgarn land-surface. Recent work by Rasmussen et al. (2012) has given a reasonably precise age of 1.89 Ga for the start of deposition. The three lowest formations of the Earaheedy Group and the underlying Archean basement were involved in the impact at Shoemaker.

Pinjarra Orogen

The Pinjarra Orogen consists of several diverse rock groups, ranging in age from Mesoproterozoic to earliest Paleozoic, that form inliers within or basement to the Perth basin. Some are known only from oil wells. Although most are to the west of the Darling Fault, several sequences form narrow belts between the Darling fault and Archean rocks of the Yilgarn Craton.

One of these sediment stacks which occurs east of the Yalallie structure is the Moora Group that occurs as a 170 km x 16 km north-south sliver east of the Darling Fault. The Moora Group consists of fluviatile-alluvial fan arenites and argillites overlain by paralic siliciclastics and dolomitic sediments, which, in turn, are overlain by a sequence of sandstone, siltstone, basalt and tuffs (Baxter and Lipple, 1985). The Moora Group is possibly up to 2 km thick, is weakly metamorphosed and has poorly constrained radiometric ages ranging from 1 Ga to 1.4 Ga. Silicified stromatolitic dolostone mined from the Moora Group at Moora is the raw material used in WA's silicon smelter at Kemerton, about 180 km south of Perth.

Perth Basin

The Perth Basin comprises a linear north-south belt that includes a sequence of sedimentary rocks up to 15 km thick that accumulated dominantly between Devonian (about 350 Ma) and late Cretaceous (65 Ma) times. The palaeoenvironment was dominated by shallow marine through nearshore to lacustrine and fluviatile systems in a north south-oriented gulf bounded to the east by the Darling Fault, to the west by the precursor to India, and to the south by the ancestral Antarctica, with the open ocean, the Tethyan Ocean, to the north. Through this period of sedimentation parts of the underlying Pinjarra Orogen slowly sank, with the sediment supply keeping pace with the sinking, and consequently the basin was not exposed to deep-water sedimentation. This is significant in respect to the Yalallie impact structure in that it occurred in a shallow marine environment.

The Perth Basin sediments are predominantly arenaceous with less-common silts and argillaceous components, widespread, but relatively thin, coal seams, limestone, and rare glacigenic sediments. Dating of zircons in the sediments implies the Perth Basin sediments were derived largely from the Mesoproterozoic Albany-Fraser Orogen or the Neoproterozoic Leeuwin Complex and with very limited supply from the adjacent Archean Yilgarn Craton (Sircombe and Freeman, 1999; Cawood and Nemchin, 2000). The importance of these findings is that they show that the surface of the Yilgarn Craton has not been eroded much during the past 250 Ma, and this, in turn, implies that there could still be a number of impact structures yet to be identified.

Figure 5: Cretaceous basalt flow at Black Point.

130 Ma basalt flows in the southern part of the basin (Figure 5) are related to the rifting off and westward movement of the Indian subcontinent, and the subsequent opening of the Perth Basin to more open ocean influences. However, the sinking of the underlying basement slowed and ceased with or soon after the rifting leading to cessation of the sediment accumulation.

During Cenozoic times the Perth Basin surface has been dominated by establishment of a series of shore-parallel sand dunes, with composition ranging from siliceous to calcareous. Rapid cementing of the lime-rich dunes had produced the Tamala Formation that is now locally cavernous and generates tourist interest. The dunes extend inland by up to 7 km from the present shoreline, and inland of those and up to the base of the Darling Scarp is low-sloping clay-dominant plain.

A series of parallel palaeoshorelines occur within the dunes dating up to 2 Ma (though the dating is ill-constrained). These contain concentrations of ilmenite, zircon, rutile, xenotime and other high-density mineral sands that constitute rich deposits of these minerals, Their existence in some very rich deposits led to the development of a world-dominant mineral sand industry where WA produced up to 75% of the worlds supplies of some of the minerals in past years. However, the richer deposits are now depleted and the industry is gradually ebbing. At Eneabba, near the Yalallie impact structure, rutile-zircon-rich deposits located in the 1960s mining is currently resurging in response to work market demand for the commodities.

Regolith

Most of Western Australia has been a very stable part of the Earth's crust for very long periods. Therefore, even though Australia is renowned as an old continent, this western part has been the epitome of age and geological stability, and has been without mountain ranges or ice ages for a very long time. This has resulted in long periods of weathering of the near surface rocks, and soils that are very old and of limited fertility. Recent dating of minerals and interpretations of regional geology suggests that the present surface of the Yilgarn Craton may date back to perhaps Permian times (250 Ma). Through this long period of exposure, there has been intense weathering and formation of lateritic profiles. These profiles are up to 100 m thick, and formed during periods partly experiencing distinctive climates. Lateritic profiles are distinctively zoned. Researchers have developed several different systems of nomenclature for the profiles, but simplistically they consist of:

- An uppermost layer of iron-rich ('ferricrete') or siliceous ('silcrete') caprock that is strong, resists further weathering and erosion and forms a hardcapping up to about 4 m thick;
- An intermediate clayey layer, up to 10 m thick, that commonly contains parts that are "mottled", with patches of iron-rich clayey material in a matrix of bleached clayey weathered material; and
- A lowermost layer that grades into the bedrock and may still retain some of the appearance of bedrock.

The laterite profile is economically important in the Darling Range southeast of Perth where the caprock constitutes the bauxite ore that provides humanity with some 20% of its aluminium, and in the goldfields it commonly contains gold or nickel which can be exploited. Laterite profiles are developed over all rock-types.

On the excursion, the lateritic profiles will be noted to characteristically form breakaways; continuous to semicontinuous lines of low cliffs topped by the caprock protecting the underlying less-resistant clayey regolith (Figure 6). The underlying material progressively weathers away, undercutting the caprock, generating shallow caves that form the habitat of various native animals, birds and insects and previously were living habitats for Aboriginals. Cave paintings are not uncommon in some localities in these caves.

Figure 6: Breakaways in the Murchison near Dalgaranga.

Soils and alluvium along watercourses are also included in the term regolith. These materials have very diverse forms and natures, and in general conceal the bedrock. They are, however, very important for life, because they are the material in which humans grow their crops.

During the early Cenozoic the West Australian climate was more pluvial and significant integrated drainage systems developed, possibly having been initiated in the late Palaeozoic. From the Pliocene onwards the climate dried. The major river systems ceased flowing and the valleys became choked with sediment either washed from surrounding slopes by intermittent runoff and eolian sands that spread across the country. Consequently the former valleys now reveal themselves as palaeovalleys ranging from short relict interconnected channels to lines of playas in vague lows through the country. Salts transported from modern ocean sprays are carried well inland and reportedly are deposited even in the Kalgoorlie region at present rates of three tonnes per hectare per annum of NaCl (Freeman, 2001). Deposition of this quantity of salt through the arid interior over prolonged times has led to the build-up of salts in the playas. Gypsum derived from both spray and from weathering of the basement rocks is common and calcrete is locally common, again derived from local arid weathering. The lines of the palaeovalleys are a dominant landscape feature throughout the interior of WA. They are particularly common in the vicinity of the Shoemaker Impact Structure.

Calcrete (Figure 7) is one of a number of pedogenic accumulations of calcium carbonate that go under a range of names, including caliche, kunkar, kankar, calcareous duricrust and others. In Western Australia calcrete is largely confined to near the axes of palaeochannels where it was precipitated from groundwaters or possibly in palaeolake environments. It is typically a cream-white, massive to vuggy rock commonly with sand- to pebble-sized clasts of nearby basement rock and in places it may have weak horizontal layering. Some calcrete occurrences are being researched as potential orebodies of uranium where groundwater deposits of carnotite have formed.

Figure 7: calcrete.

References

Baxter, J. L., and Lipple, S. L., 1985 . Perenjori, WA. Geological Survey of Western Australia 1:250 000 Geological Series Explanatory Notes.

Cawood, P. A. and Nemchin, A. A., 2000. Provenance record of a rift basin: U/Pb ages of detrital zircons from the Perth Basin, Western Australia. Sedimentary Geology, 134, p. 209-234.

Freeman, M. J., 2001. Avon River Paleodrainage System, Western Australia: geomorphological eveolution and environmental issues related to geology. In: V. A. Gostin (Ed), Gondwana to Greenhouse. Australian Environmental Geoscience, Geolgical Society of Australia Special Publication 21, p. 37-47.

Halilovic, J., Cawood, P.A., Jones, J.A., Pirajno, F. and Nemchin, A.A., 2004. Provenance of the Earaheedy Basin: implications for assembly of the Western Australian Craton. Precambrian Research, 128, 343-366.

Hickman, A. H., 2012. Review of the Pilbara Craton and Fortescue Basin, Western Australia: crustal evolution providing environments for early life. Island Arc, 21, p. 1-31.

Johnson, G. I., 1991. The petrology, geochemistry and geochronology of the felsic alkaline suite of the eastern Yilgarn Block, Western Australia: The University of Western Australia PhD Thesis (unpublished).

Johnson, S. P., Thorne, A. M., Cutten, H. N., Tyler, I. M., and Blay O., 2011. Geology of the Gascoyne Province. In: Johnson, S.P., Thorne, A.M., and Tyler, I.M., (Eds) Capricorn Orogen seismic and magnetotelluric (MT) workshop 2011: extended abstracts. Geological Survey of Western Australia Record 2011/25.

Pirajno, F., Jones, J. A., and Hocking, R. M., 2004. Geology of the Nabberu and Granite Peak 1:100 000 Sheets. Geological Survey of Western Australia, 1:100 000 Geological Series.

Rasmussen, B., Fletcher, I. R., Bekker, A., Muhling, J. R., Gregory, C. J. and Thorne, A. M., 2012. Deposition of 1.88-billion-year-old iron formations as a consequence of rapid crustal growth. Nature, 484, p 498-501.

Sircombe, K. N. and Freeman, M. J., 1999. Provenance of detrital zircons on the Western Australian coastline - implications for the geologic history of the Perth Basin and denudation of the Yilgarn Craton. Geology 27, p. 879-881.

Thorne, A. M., Johnson, S. P., Cutten, H.N., and Blay, O., 2011. Structural development and mineralization of the western Edmund and Collier Basins, In: Capricorn Orogen seismic and magnetotelluric workshop 2011: extended abstracts. Geological Survey of Western Australia Record 2011/125.

Trendall, A. F., and Blockley, J. G., 1970. The iron formations of the Precambrian Hamersley Group, Western Australia. Geological Survey of Western Australia Bulletin 119.

Tyler, I. M., 1994. Geology of the Newman 1:100 000 Sheet. Geological Survey of Western Australia, 1:100 000 series Explanatory Notes.

Wilde, S. A., Valley, J. W., Peck, W. H., Graham, C. M. and Collin, M., 2001. Evidence from detrital zircons for the existence of continental crust and oceans on the Earth 4.4 Gyr ago. Nature, 409 (6816), p. 175-178.

Wyche, S., Nelson, D.R. and Riganti, A., 2004. 4350-3130 Ma detrital zircons in the Southern Cross Granite-Greenstone Terrane, Western Australia: implications for the early evolution of the Yilgarn Craton. Australian Journal of Earth Sciences, 51, p. 31-45.

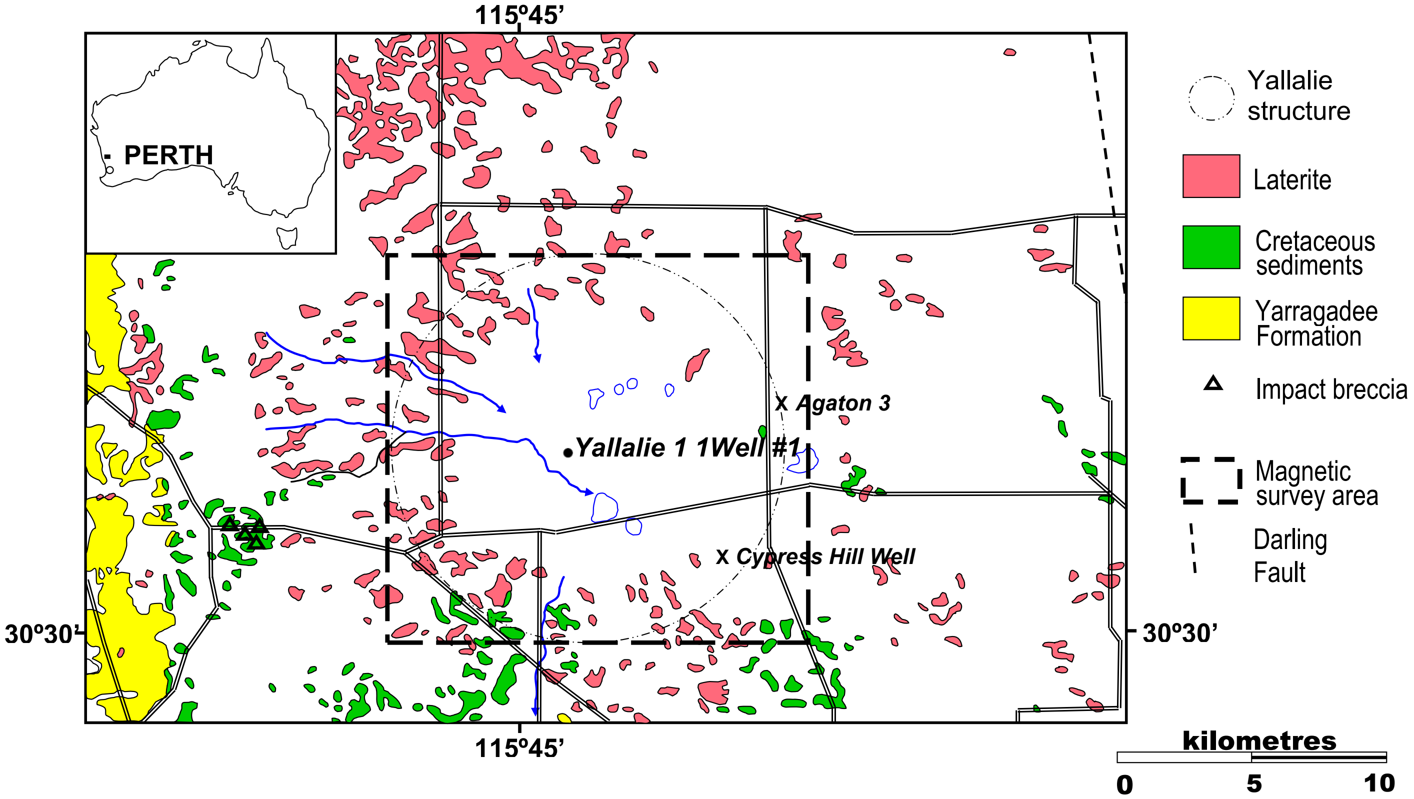

Figure 1: Geological map of the Yallalie area showing the location of the structure and other key features.

Yallalie Impact Structure

Alex Bevan

An anomalous buried, circular structure in Mesozoic sedimentary rocks in the Dandaragan Trough of the Perth Basin, Western Australia was discovered during exploration for oil in 1990, and described subsequently by Dentith et al. (1999) as of possible impact origin. The Yallalie structure (centred on 30˚ 26’ 40.3”S., 115˚ 46’ 16.4”E) is about 12 km in diameter (Figure 1). Seismic profiles show a basin of chaotic reflections extending to a depth of ca. 2 km. The structure is characterised by a centrally uplifted region, approximately 3-4 km across, similar to those described from complex impact structures. Quartz grains from the Yallalie 1 well that penetrated the central uplift show the development of prismatic cleavage fractures indicative, but not diagnostic of low shock levels. However, definitive evidence of an impact origin for the structure in the form of multiple sets of closely spaced planar deformation features (PDF’s) in quartz or feldspar has yet to be observed in the rocks of the structure. Notwithstanding, the morphology of the Yallalie structure suggests that it is of impact origin (Dentith et al.,1999; Hawke, 2003).

An anomalous, polymictic, allochthonous breccia of Jurassic and Cretaceous rocks occurs adjacent to the structure at Mungedar (30˚ 28’S, 115˚ 39’E), and lies adjacent to a sequence of faulted but otherwise undisturbed rocks of Jurassic and Cretaceous age. Dentith et al. (1999) suggested that this breccia, informally named the Mungedar Breccia, is related to the Yallalie structure, and is also of impact origin.

Geological setting

The Perth Basin is a major rift basin nearly 1000 km long, and averaging 65 km in width (Playford et al., 1976). The eastern margin of the Perth Basin is truncated by the Darling Fault, which has an estimated downward throw of more than 10 km to the west. Archaean and Proterozoic rocks of the Yilgarn Craton are exposed to the east of the Darling Fault. The Perth Basin formed in a rift that led to the continental breakup of Gondwana, commencing in Cretaceous times. Deposition commenced in the Silurian to early Permian as an intracontinental rift basin, with major fault development continuing until the separation of India from Australia during the Early Cretaceous. The Dandaragan Trough is one of the major depocentres of the onshore Perth Basin containing up to 12 km of Permian and Mesozoic sediments (Mory and Iasky, 1996).

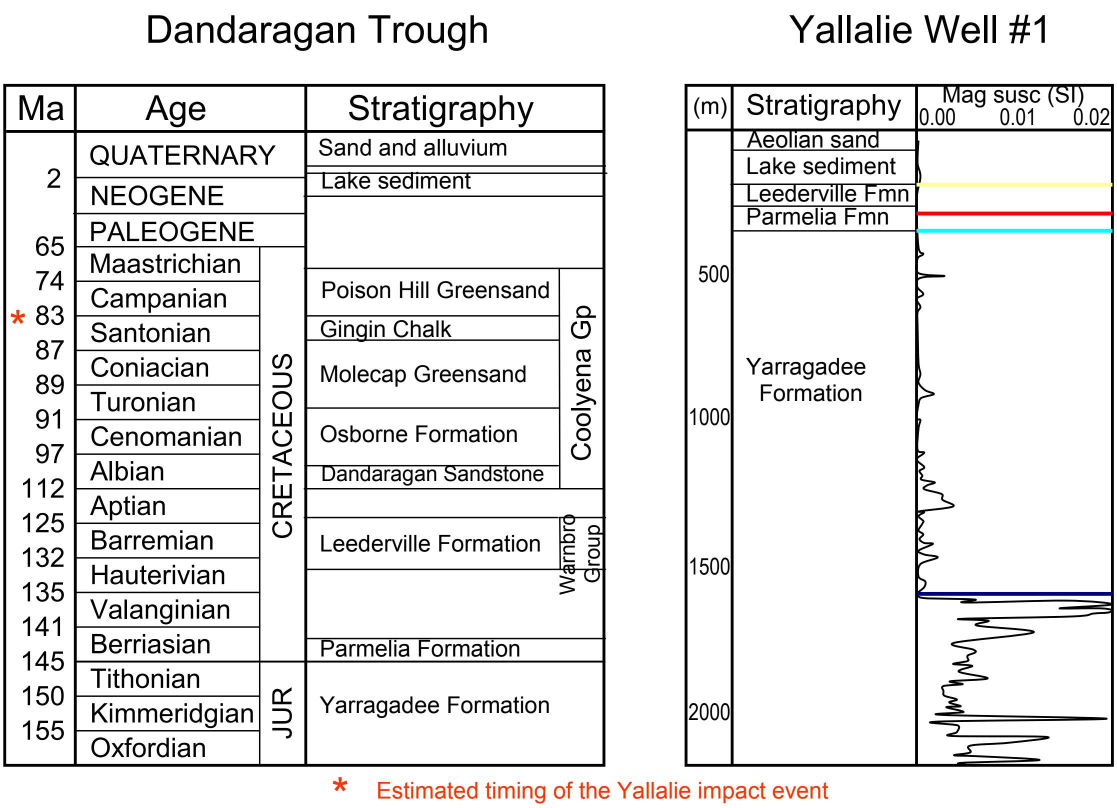

Figure 2: Stratigraphy of the Dandaragan Trough compared with that encountered in the Yallalie Well 1 borehole.

The Mesozoic and Cenozoic stratigraphy of the Dandaragan Trough in the area near Yallalie is shown in Figure 2, compared with the stratigraphy of the Yallalie 1 well drilled through the centre of the Yallalie structure. In the Dandaragan Trough, the Jurassic stratigraphy consists of a thick sequence of continental sedimentation including the Eneabba Formation, Cattamarra Coal Measures and the Yarragadee Formation, separated by a relatively thin marine unit, the Cadda Formation. The Cattamarra Coal Measures comprise fluvio-deltaic sandstone, siltstone and claystone more than 1000 m thick and contain carbonaceous material including coal seams. The Cadda Formation is a mix of fossiliferous, shallow marine, calcareous sediments and limestone. In the Dandaragan Trough, the thickness of the Cadda Formation is estimated to be between 150 and 250 m (Mory and Iasky, 1996). The Yarragadee Formation is a thick (ca. 3000 m) sequence of feldspathic sandstones, with siltstone and claystone, and minor seams of coal, deposited in a fluviatile to lacustrine environment.

The Yarragadee Formation is succeeded conformably by the Parmelia Formation (Early Cretaceous), which is a clastic sedimentary sequence similar to the Yarragadee Formation. The basal Otorowiri Member is largely siltstone and was probably deposited in a lacustrine environment. A prominent seismic horizon within the upper part of the Parmelia Formation may be a thick siltstone, or claystone layer, within the Carnac Member.

The Early Cretaceous Warnbro Group overlies the Parmelia Formation unconformably and is interpreted to be the first sedimentary unit to be deposited after the separation of India from Australia. The Warnbro Group consists of shallow marine to fluvial sediments up to 800 m thick. Two formations are identified elsewhere in the Perth Basin, the South Perth Shale and the Leederville Formation. Regional drilling (Moncrieff, 1989) suggests that only the Leederville Formation is preserved within the Dandaragan Trough and is approximately 250 m thick. The Leederville Formation comprises interbedded sandstone, siltstone and claystone, containing some glauconite and pyrite.

The Warnbro Group is succeeded unconformably by the Coolyena Group. Four units, the Osborne Formation (including the Dandaragan Sandstone), Molecap Greensand, Gingin Chalk and Poison Hill Greensand form a succession that is overall less than 150 m thick. The sequence is contiguous with the Lancelin Formation of Maastrichtian age near the coast (McNamara et al., 1988; Mory and Iasky, 1996).

Pliocene lake sediments above the Yallalie structure are the only Neogene deposits in the Dandaragan Trough. A thin veneer of laterite has formed over the surface of much of the Perth Basin, including the Dandaragan Trough, locally obscuring the older stratigraphy. Laterite may have formed during several intervals in the Cenozoic, although a major period of lateritisation is thought to have occurred during the Pleistocene (Playford et al., 1976).

Most of the surface geology surrounding the Yallalie structure is mapped as Late Cretaceous rocks of the Coolyena Group capped by laterite. However, to the west and south of the Yallalie structure there are also extensive outcrops of the Yarragadee Formation, which also includes what is now recognised as the Parmelia Formation. The broad, circular depression representing the present day surface expression of the Yallalie structure is a centre for drainage which flows centripetally into the structure. Springs rise on the 'rim' of the depression and flow all year round. The Yallalie structure is concealed beneath unconsolidated Quaternary alluvium and aeolian sand.

While the Yallalie structure is best defined from the seismic data (Figure 3), stratigraphic control within the structure is provided by two petroleum exploration wells, Yallalie 1 (Economo, 1991) and Cypress Hill 1 (Higgins, 1988). The Yallalie structure and surrounding area was also drilled for water by the Agaton Borefield exploratory programme (Passmore, 1969). The Yallalie 1 well (Economo, 1991) was drilled into the centrally uplifted region of the Yallalie structure. However, this borehole was not continuously cored, and contacts were largely predicted from wireline logging, assisted by palynological interpretation of a limited number of sidewall cores. The top 177 m of the drill hole intersected lake sediments and sand. This section of the borehole was subsequently redrilled by continuous coring from the base of the sand at 66m depth as Yallalie 2 (Dodson and Ramrath, 2001). Palynological analysis of the lake sediments provide an age of mid-Pliocene, between 2.5 and 3.5 Ma. The unconformity with the Cretaceous is marked by a distinctive colour change indicating a period of weathering or leaching (Economo, 1991), suggesting that the central uplift has undergone at least one period of weathering and erosion.

The youngest possibly deformed sedimentary rock in the Yallalie 1 well is a sequence of claystone, sandstone and coal intersected between 177 and 139 m, which is identified by palynology as the Leederville Formation. However, J. Backhouse (pers. comm.) has noted a significant reworking of the microfossils recovered from this section, indicating that this sequence may represent eroded and redeposited material or, possibly, an impact breccia. The latter interpretation, however, lacks the supporting evidence of the recognition of shock metamorphic features. A thinned sequence of Parmelia Formation was intersected between 239 to 312 m overlying the upper 3000 m of Yarragadee Formation. Wireline logging of the Yallalie 1 well indicates that the base of chaotic disruption of beds occurs at a depth of approximately 1560 m.

The Cypress Hill 1 well was drilled on a rotated fault block near the inner margin of the Yallalie structure (Figure 1). This drill hole was not continuously cored, and stratigraphic interpretation is primarily from wireline logging aided by palynology of some sidewall cores. Below 38 m of aeolian sand, the well intersected 308 m of sandstone with minor claystone and coal, interpreted as the Leederville Formation, and almost the entire sequence of Parmelia Formation (588 m). The Cyprus Hill 1 well did not intersect the Yarragadee Formation. Stratigraphic control at the margin of the structure, and outside it, is provided by the Agaton 3 borehole situated on the rim of the structure, the Dandaragan 1 well, located 18 km to the south of the centre of Yallalie, and the Warro 2 well situated 40 km to the north.

The Agaton 3 borehole intersected 146 m of sandstone which has been reinterpreted as Dandaragan Sandstone (Osborne Formation) overlying 220 m of Leederville Formation. The bore terminates in sandstone and siltstone of the Parmelia Formation. The stratigraphic uplift at the centre of the Yallalie structure is estimated by the vertical displacement of the Otorowiri Member of the Parmelia Formation. A structural uplift of 690 m is measured from the relative level (RL) difference between the base of the Parmelia Formation in the Cypress 1 and Yallalie 1 wells and other wells outside the structure. This matches closely the structural uplift (700 m) estimated by Dentith et al. (1999). In contrast, only a small amount of uplift is apparent in the overlying Leederville Formation. This supports the interpretation that this stratigraphic interval in Yallalie 1 actually represents reworked material.

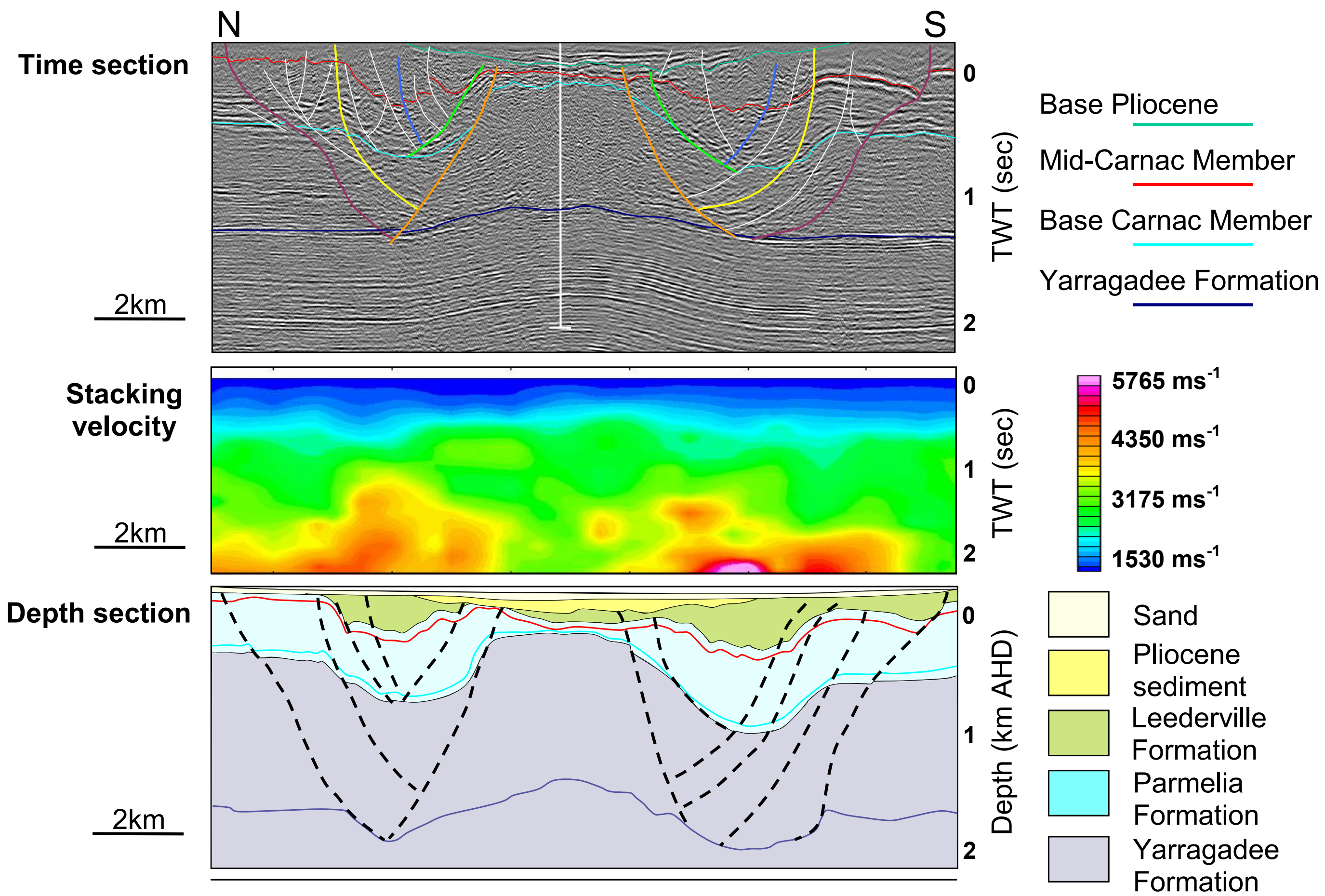

Fig 3: Two-way time (TWT) seismic section of the Yallalie structure (the central vertical line is the Yallalie 1 well) with interpretation and stacking velocity section used to produce the approximate depth corrected geology section.

The region at Mungedar occupied by the breccia may preserve an original Cretaceous surface (sea bed?) on to which the breccia was deposited. The source of the rounded quartzite boulders in the Mungedar Breccia is enigmatic. Similar boulders are occasionally to be found embedded in the Quaternary sands and gravels overlying the Yallalie structure. This lithology does not match any in the sequence of Jurassic or Cretaceous rocks in the Dandaragan Trough. It is possible that the quartzite boulders were eroded from the Archaean and Proterozoic rocks of the Yilgarn Block which lies just to the east of the Yallalie structure, and which represents a former coastline. Alternatively they represent material that has become deeply silicified as the result of lateritization.

The Mungedar Breccia resembles the famous Bunte Breccia (Hörtz et al., 1983) associated with the 15.1 Ma Ries impact crater (26 km in diameter) in Germany. At Ries, large amounts of ejecta are preserved, including both the Bunte Breccia and the overlying suevite. Locally the ejecta is more than 100 m thick. Similar to the Bunte Breccia, the Mungedar Breccia appears to lack any obvious vertical stratification. However, this breccia is a vestige of what may have been originally a thicker and more extensive deposit, and it covers a much smaller area than the Ries Bunte Breccia. The limited extent of the Mungedar Breccia, and its proximity to the crater (<4 km) suggests that it is unlikely that an inverted stratigraphy could be demonstrated in the breccia. However, the flow directions running parallel with the ridges and pointing away from the crater suggest a causal relationship with the impact event, and support the suggestion that the breccia was emplaced as a ground-hugging, turbulent surge deposit.

Geophysics and interpretation of the Yallalie structure

Seismic data

The Yallalie structure appears as a roughly bowl-shaped area of disrupted seismic character. This zone of disruption extends to about 1.5 s two-way time (TWT), roughly 1500 m below the surface. A sharp contact between the Yallalie structure and the surrounding undisturbed sedimentary strata appears to form a normal listric fault. This fault is consistent with the slumping expected at the outer margins of a complex impact crater and is interpreted to define the outer extent of the collapsed crater. The fault, at a radial distance of 4.2 km from the centre of the Yallalie structure is also interpreted as slumping in the outer terraced terrain of the crater. Another fault, primarily identified from magnetic data, bounds an area approximately 6 km in diameter. The limit of coherent reflectors in the outer part of the Yallalie structure is interpreted to be between the two faults. Two sets of listric faults, with an apparently normal sense of movement form the central uplift of the structure. The inner fault is linked to what was probably once the floor of the transient cavity at 1.5 s TWT (1500 m). The outer fault bounds dipping reflectors that define the outer extent of the centrally uplifted area (Figure 3).

Magnetic data

An airborne magnetic and radiometric survey (Figure 4) was commissioned over an area approximately 14 km^2 centred on the Yallalie structure (Hawke, 2004, unpublished). Generally, sediments in the Perth Basin are non-magnetic (<50 x 10-5 SI). An obvious exception to this are the magnetic intervals intersected in Yallallie 1. No magnetic unit was intersected in the Cypress Hill 1 borehole. While the water exploration well Agaton 2 was ideally situated to test the main circular magnetic anomaly in the Yallalie structure, cuttings from this borehole are not retained by the Geological Survey of Western Australia.

Several sub-circular, concentric, positive magnetic anomalies, centred on a single magnetic peak near the middle of the Yallalie structure, are clearly evident in the magnetic data. The outermost magnetic anomaly is roughly 12 km in diameter, and closely matches the extent of the structure interpreted from seismic data. An excellent correlation can be made between faults identified in the interpretation of seismic data with the location of circular magnetic anomalies (Figure 5). The inner margin of the main circular magnetic anomaly, with a diameter of 3.4 km, correlates with the extent of the crater's central uplift. A detachment fault within the central uplift, interpreted from the seismic data, describes an area a little bigger than the central magnetic peak. The outer margin of this anomaly compares closely with a second order fault that has a diameter of 6 km and is interpreted to be an estimate of the extent of the transient cavity. Weaker magnetic rings, with diameters of 8.8 km and, possibly 10 km are interpreted to be related to slump structures in the outer terraced terrain of the structure. Several small cross-terraces are also evident. There is also a fault marking the outer margin of the collapsed structure. Several small-scale faults, due to continued

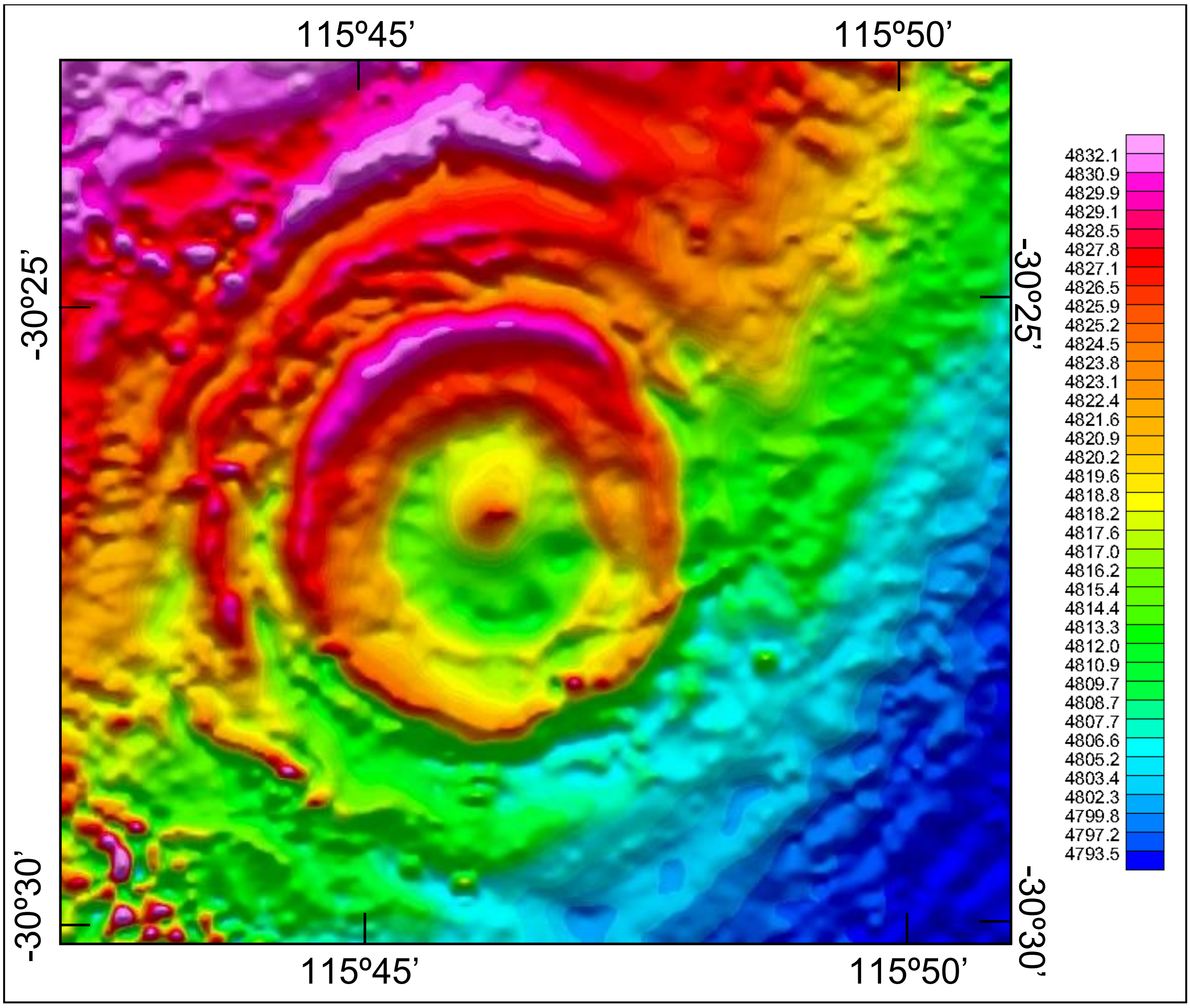

Figure 4: Total magnetic intensity from an airborne geophysical survey over the Yallalie structure.

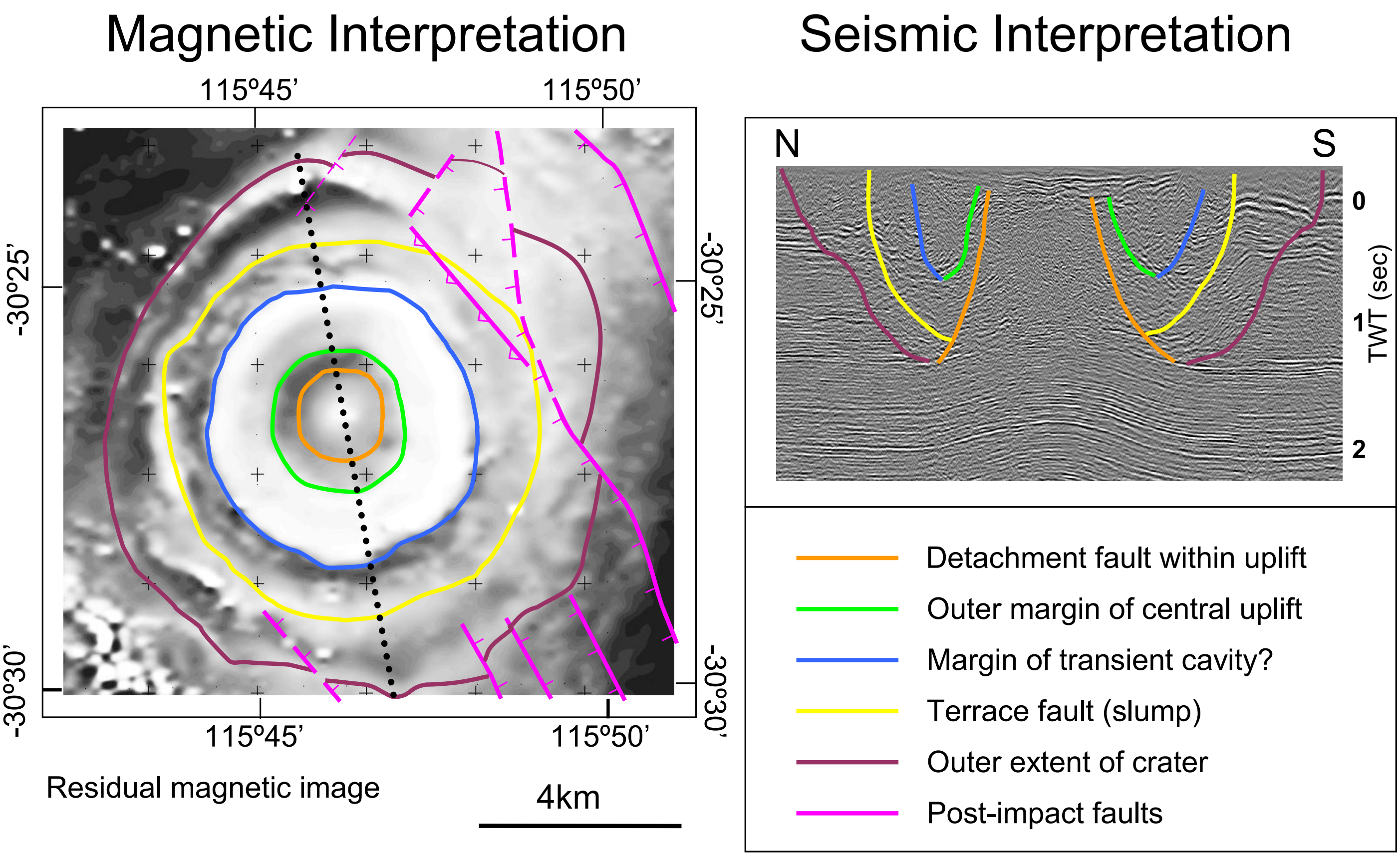

Figure 5: Correlation of magnetic and seismic data. Structural interpretation from seismic data overlain on a grey-scale image of the polynomial residual of the magnetic data.

subsidence and deformation of the Perth Basin after the formation of the Yallalie structure can also be interpreted from the magnetic data. While these features are difficult to identify amongst the disrupted seismic character within the structure, they can be mapped from offsets in the circular magnetic anomalies. The concentric magnetic anomalies coincident with faults in the Yallalie structure define what were originally highly terraced interior crater walls. The source of the magnetic anomalies remains uncertain. Geophysical modelling indicates that the source of the concentric magnetic anomalies lies at a depth of around 130 m. Although no particular lithological source has been identified, the depth rules out post-impact sediments as the source. The most plausible explanations of the magnetic anomalies are that they may be related to structurally controlled, post-impact hydrothermal alteration that led to the deposition of magnetic mineral species, or impact breccias containing suevites.

Gravity data

Gravity data have been collected over the Yallalie structure and surrounding areas at various times. Data extracted from Geoscience Australia's gravity database were used as the base level to tie all other surveys, and include the 11 km spaced stations regional data acquired by the former Bureau of Mineral Resources (BMR) (now Geoscience Australia), and several detailed traverses across the Darling Fault. Five detailed gravity traverses were collected for Ampol Exploration soon after the discovery of the Yallalie structure (Frankcombe, 1989, 1990). Additional gravity data were acquired over an area of approximately 45 x 52 km in two stages, during May and December 2000 (Hawke, 2004, unpublished). One of the primary aims of this survey was to define the strong regional gravity field due to the Darling Fault, allowing the response associated with the Yallalie structure to be separated.

The gravity field of the Dandaragan Trough has a dynamic range of over 130 mGals. This gravity response mainly reflects the thickness of sedimentary rocks within the Perth Basin, with the maximum gradient of the north-south trending gravity high roughly defining the position of the Darling Fault. Increased gravity towards the western margin of the survey area is related to an Archaean basement high, Beagle Ridge, that defines the western margin of the Dandaragan Trough. A small flexure in the gravity field near the centre of the Dandaragan Trough coincides with the position of the Yallalie structure. The exact nature of this feature is difficult to resolve because of the strong regional gravity field, which forms a local gradient of almost 2 mGal/km at Yallalie. As the regional gravity field roughly approximates the thickness of sediment within the Dandaragan Trough, it forms a broad, low gravity trough that has its centre near the Yallalie structure. This complex field is difficult to isolate and remove from the small positive anomaly that represents the Yallalie structure.

The application of a simple 2.5D forward model was used to remove the effects of the strong regional field across the Dandaragan Trough. The margins of the Perth Basin sedimentary layers are interpreted to be fault bounded; by the Darling and Urella Faults on the eastern margin of the Dandaragan Trough and a structure controlling the development of the Beagle Ridge at the western end of the modelled section. A close match for the regional gravity field across an east-west traverse was achieved with this model. The small positive gravity high coincident with the Yallalie structure becomes higher than the background response at a diameter of 16.5 km, 35% greater than the rim diameter defined from the seismic data. This is contradictory to the expected gravity signature over an impact structure, which, although variable, is generally negative (Grieve and Pilkington, 1996). With a portion of the ejecta layer preserved just outside the crater rim, Yallalie is probably not very deeply eroded. Therefore, it is reasonable to expect that impact breccias are still preserved within the structure, beneath the layer of post-impact sediments. Hence the gravity anomaly is unlikely to be due simply to the removal of lowered density material.

The positive gravity signature at Yallalie with a maximum amplitude of between 5.5 and 6.0 mGal, unusual for a sedimentary target, most probably represents a density increase resulting from a decrease in porosity by the removal of volatiles from the target rocks during shock-loading.

Age

Within the central uplift of the Yallalie structure the entire Late Cretaceous Coolyena Group is missing, whilst undisturbed sequences of these rocks outcrop adjacent to the structure. It is reasonable to assume then, even with the uncertainties in the age of the structure, that some, if not all, of these lithologies formed part of the target rocks.

Assuming a causal relationship, the allochthonous breccia provides the only evidence of the age of the Yallalie structure. Attempts to determine the age of the clasts in the Mungedar Breccia by palynology are severely hampered by deep weathering. However, several competent lithologies have been tentatively identified as the Molecap Greensand, Dandaragan Sandstone, and siltstones and shales of the Yarragadee Formation. The apparent absence of a distinctive and easily recognisable lithology such as the Gingin Chalk from the Mungedar Breccia suggests that breccia formation might have pre-dated the deposition of this lithology. However, environments for chalk deposition can be very localised. The age of the breccia, and therefore the impact event, is consequently bracketed between the Gingin Chalk (Santonian) and the Poison Hill Greensand (Campanian) (Bevan et al., 2004).

Environment of impact

Many of the features of the Yallalie structure, such as the pronounced central uplift and the remnants of what might have been once highly terraced, interior crater walls now marked by magnetic anomalies, strongly suggest impact into volatile-rich target rocks (French, 1998). The Coolyena Group represents a continuous sequence of marine to shallow marine (neritic) deposition in approximately less than 100 m of water. The Molecap Greensand contains abundant fossil wood and rare dinosaur remains indicating shallow, nearshore deposition. If the estimated age of the Yallalie structure is correct, then it is very likely that the impact occurred into a shallow marine environment.The evidence (morphometric and petrological) strongly suggests, therefore, that the impact at Yallalie took place into volatile-rich, perhaps water-saturated rocks. However, whether the impact was subaqueous or subaerial is less certain. Most of the features of the Yallalie structure, including final confirmation of its impact origin, will not be resolved until further drilling within the structure, and additional drilling within the Mungedar Breccia, has been undertaken.

Locality 1 is at a dam on a Mungedar property, at the junction between the North West Road and Mungedar Road: 30°28'8.91"S 115°39'40.9"E

Locality 1: Mungedar Breccia

The aerial extent of the Mungedar Breccia is limited to approximately 2 km^2 and, although highly variable, its maximum thickness is estimated from contours and exposures to be around 30 metres. Low, elongated ridges of breccia running approximately ENE-WSW occupy a region approximately 4 km from the south-western 'rim' of the Yallalie structure.

In detail, the breccia comprises material varying in size from mega-blocks measuring several metres across, to clasts of no more than a few centimetres to a few tens of centimetres across that are set in a fine-grained, clastic 'matrix' that sometimes shows textural evidence of fluidisation. The matrix has a distinctive greenish-brown colour resulting from abundant glauconite. Overall, there does not appear to be any obvious vertical stratigraphic variation within the breccia which is a chaotic mixture of rock types and clast sizes.

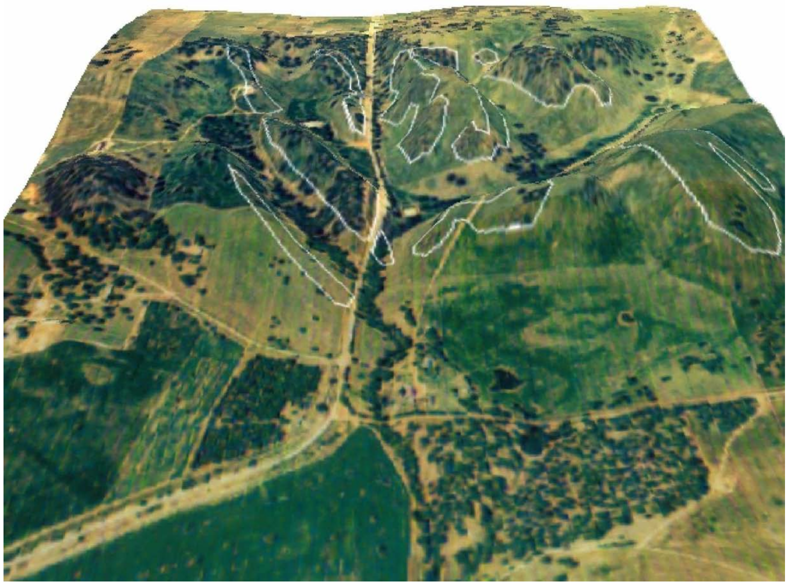

Figure 6: Approximate areal extent of the Mungedar Breccia. Outcrops are mapped on a perspective view created by draping an aerial image over a high-resolution digital elevation model, viewed towards the east, and the rim of the Yallalie structure. The image shows that the breccia outcrops occur along six main ridges, mainly trending towards the centre of the Yallalie structure.

The breccia outcrops occur along six main ridges (Figure 6), mainly trending towards the centre of the Yallalie structure, although the breccia and the 'rim' of the basin underlain by the Yallalie structure are separated physically by a generally flat erosional divide. The breccia does not appear to have been deposited as discrete 'lobes'. From the geomorphology, it is more likely that

Figure 7: Mungedar Breccia in outcrop.

the breccia was deposited as a single sheet that has been subsequently dissected by the modern drainage system. Rocks that might lie below the breccia are exposed in the walls of two dams near the western extent of the Mungedar Breccia. Gingin Chalk, containing fossils indicating the upper part of this deposit, is exposed at the western end of one ridge. The Molecap Greensand is found in the walls of a second dam located near the base of this ridge. At two localities the breccia is clearly capped by a thin (approximately 5 m) coherent layer of iron-stained sandstone, which may be the Poison Hill Greensand.

Unlike the other sediments in the area, the base of the breccia surface is not flat-lying, but becomes deeper towards the centre of the drainage system. There is an apparent undulation in the layers of Cretaceous stratigraphy. This may reflect the deposition of these units on a hummocky sea floor, or be related to faulting associated with the formation of the Yallalie structure. The relationship of the Mungedar Breccia to the Poison Hill Greensand, however, has not been established unambiguously.

Excursion localities

Vehicles will be parked at Locality 1: 30°28'33.57"S 115°39'40.90"E. We will walk to various ejecta outcrops.

Locality 1a: Ejecta exposed in a dam on Mungedar Farm

Good outcrops of the ejecta will be examined at a dam on the property (Figure 8). The Mungedar Breccia is composed predominantly of mega-blocks of quartzite, some of which are rounded, a pale sandstone, a green-coloured rock now largely weathered to clay, and clasts of green, glauconitic sandstone, a grey siltstone, a ferruginous, coarse-grained sandstone, a pale fine conglomerate, and a white, sometimes porcelaneous clay. The breccia also contains mega-blocks of pale, competent sandstone up to 2 metres in diameter, sometimes exhibiting large-scale conchoidal fractures and quartz veining.

Figure 8: Mungedar Breccia in outcrop showing polymict nature of clasts and flow structure. FOV: approx 1 metre.

Clasts in the Mungedar Breccia are set in a generally greenish or brown, sandy ‘matrix’, although it is likely that this is actually the finest comminuted fraction of the breccia. Many sedimentary clasts are severely deformed and smeared, indicating that they were partially consolidated when they were incorporated into the breccia (Figure 8). Abundant flow structures are also evident in the ‘matrix’. On the small scale, the matrix of the breccia shows pronounced flow structures around what were more competent clasts, indicating an original mixture of consolidated and semi-consolidated rocks. However, other clasts were clearly derived from more competent lithologies.

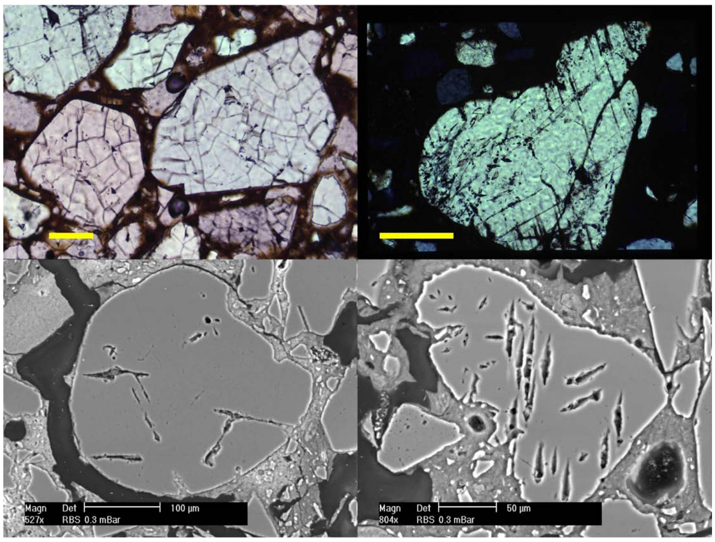

Figure 9: Quartz grains from clasts in the Mungedar Breccia variably showing brittle fracture (top left), and the incipient development of planar features indicative, but not diagnostic, of the lower levels of shock metamorphism. Scale bars 100 µm unless otherwise stated.

At the microscopic level many grains of quartz within clasts, and also in the ‘matrix’ show extensive brittle fracture, and occasionally the incipient development of planar features (PF’s) indicative of the lower levels of shock metamorphism (Figure 9), but are also known from tectonic deformation. Grains of quartz or feldspar displaying multiple sets of closely spaced PDF’s have yet to be observed in the rocks of the breccia. The highly fluidised nature of the matrix is seen in the strong alignment of mineral grains, and the presence of occasional vesicles.

From the dam we walk to adjacent outcrops of breccia.

Locality 1b: Ejecta outcrops on Mungedar Farm

The hills around the Yallalie structure are generally peneplained. It appears that the Mungedar Breccia has been preserved because it occupies, and largely fills a topographic low. It is likely that the origin of this valley predates the emplacement of the breccia. The alternative that the breccia scoured the feature in soft sediment during its emplacement is less likely, but not impossible.

Figures 10a and 10b: Mungedar Breccia in outcrop showing typical weathered appearence.

Weathered outcrops of the ejecta have a characteristic irregular outline and much of the iron has been heavily oxidised (Figures 10a and 10b).

The next stop is on the margin of the Yallalie structure, at the junction between Coalara Road and Coomberdale West Road: 30º28’08.91”S 115º43’34.53”E.

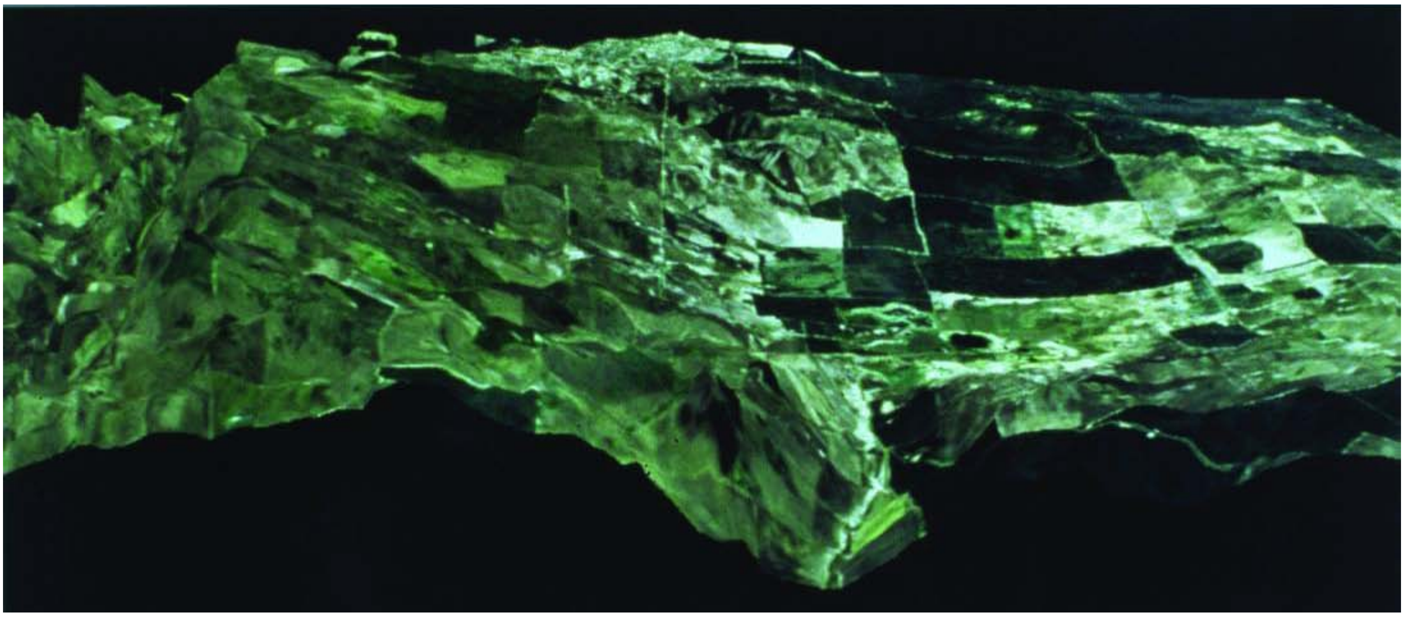

Figure 11: A perspective view created by draping an aerial image over a high-resolution digital elevation model, viewed towards the north. Vertical scale exaggerated. Image: DOLA.

Locality 2: Vista across the Yallalie Impact Structure

Looking eastwards it is possible to make out the shallow, bowl-shaped surface expression of the structure (Figure 11, and see also Figure 1). The depression is partially filled by Pliocene lake sediments and there are marshy areas in the centre. Drainage is radial into the depression.

References

Bevan, A. W. R., Hough, R. M. and Hawke, P., 2004. Morphology and origin of an allochthonous breccia near the Yallalie structure, Western Australia: Evidence for subaqeous impact? Geological Society of Australia Abstracts 73, 17th Australian Geological Convention, Hobart, 227.

Dentith, M. C., Bevan, A. W. R., Backhouse, J., Featherstone, W. E. and Koeberl, C. 1999. Yallalie: a buried structure of possible impact origin in the Perth Basin, Western Australia. Geological Magazine, 136, 619-632.

Dodson, J. R. and Ramrath, A., 2001. An Upper Pliocene lacustrine environmental record from south Western Australia - preliminary results. Palaeogeography, Palaeoclimatology, Palaeoecology, 167, 309-320.

Dypvik, H. & Jansal. F., 2003. Sedimentary signatures and processes during marine bolide impacts: a review. Sedimentary Geology, 161, 309-337.

Economo, M. 1991. Perth Basin EP 321, Western Australia, Yallalie No. 1 Well Completion Report.. Ampol Exploration Ltd. (unpublished).

Frankcombe, K., 1989. Goonderoo gravity survey. World Geoscience Report prepared for Ampol Exploration (unpublished).

Frankcombe, K., 1990. Sangaree gravity survey. World Geoscience Report prepared for Ampol Exploration (unpublished).

French, B. M., 1998. Traces of Catastrophe: A Handbook of Shock-Metamorphic Effects in Terrestrial Meteorite Impact Structures. LPI Contribution No. 954. Lunar and Planetary Institute, Houston, 120pp.

Grieve, R. A. F. and Pilkington, M., 1996. The signature of terrestrial impacts. AGSO Journal of Australian Geology & Geophysics, 16, 399-420.

Hawke, P. J., 2004. PhD Thesis (unpublished), University of Western Australia.

Hawke, P. J., Buckingham, A. J. and Dentith, M. C., 2003. Origin of the magnetic anomalies associated with the Yallalie impact structure, Perth Basin, Western Australia. ASEG 16th Geophysical Conference and Exhibition, Adelaide, Extended Abstracts.

Higgins, R., 1988. Cypress Hill 1 - Well completion report for Ampol Exploration Ltd (unpublished).

Horz, F., Ostertag, R., and Rainey, D. A., 1983. Bunte breccia of the Ries: Continuous deposits of large impact craters. Reviews of Geophysics and Space Physics, 21, 1667-1725.

McNamara, K. J., Rexilius, J.P., Marshall, N. G. and Henderson, R. A., 1988. The first record of a Maastrichtian ammonite from the Perth Basin, Western Australia, and its biostratigraphical significance. Alcheringa, 12, 163-168.

Moncrieff, J. S., 1989. Hydrogeology of the Gillingarra borehole line, Perth Basin. Geological Survey of Western Australia Report, 26, 105-126.

Mory, A. J. and Iasky, R. P., 1996. Stratigraphy and structure of the onshore northern Perth Basin, Western Australia. Geological Survey of Western Australia Report 46, 101pp.

Passmore, J. R., 1969. Exploratory Drilling - Agaton Project, Watheroo Area Preliminary Report. Geological Survey of Western Australia Annual Report for 1968, p.12-14.

Playford, P. E., Cockbain, A. E. and Low, G. H., 1976. Geology of the Perth Basin Western Australia. Geological Survey of Western Australia Bulletin 124, 311 pp.

Poag, C. W., Plescia, J. B. and Molzer P. C., 2002. Ancient impact structures on modern continental shelves: The Chesapeake Bay, Montagnais, and Toms Canyon craters, Atlantic margin of North America. Deep-Sea Research II 49, 1081-1102.

Therriault, A. M., Grieve, R. A. F. and Reimold, W. U., 1997. Original size of the Vredefort structure: implications for the geological evolution of the Witwatersrand Basin. Meteoritics and Planetary Science, 32, 71-77.

Notes

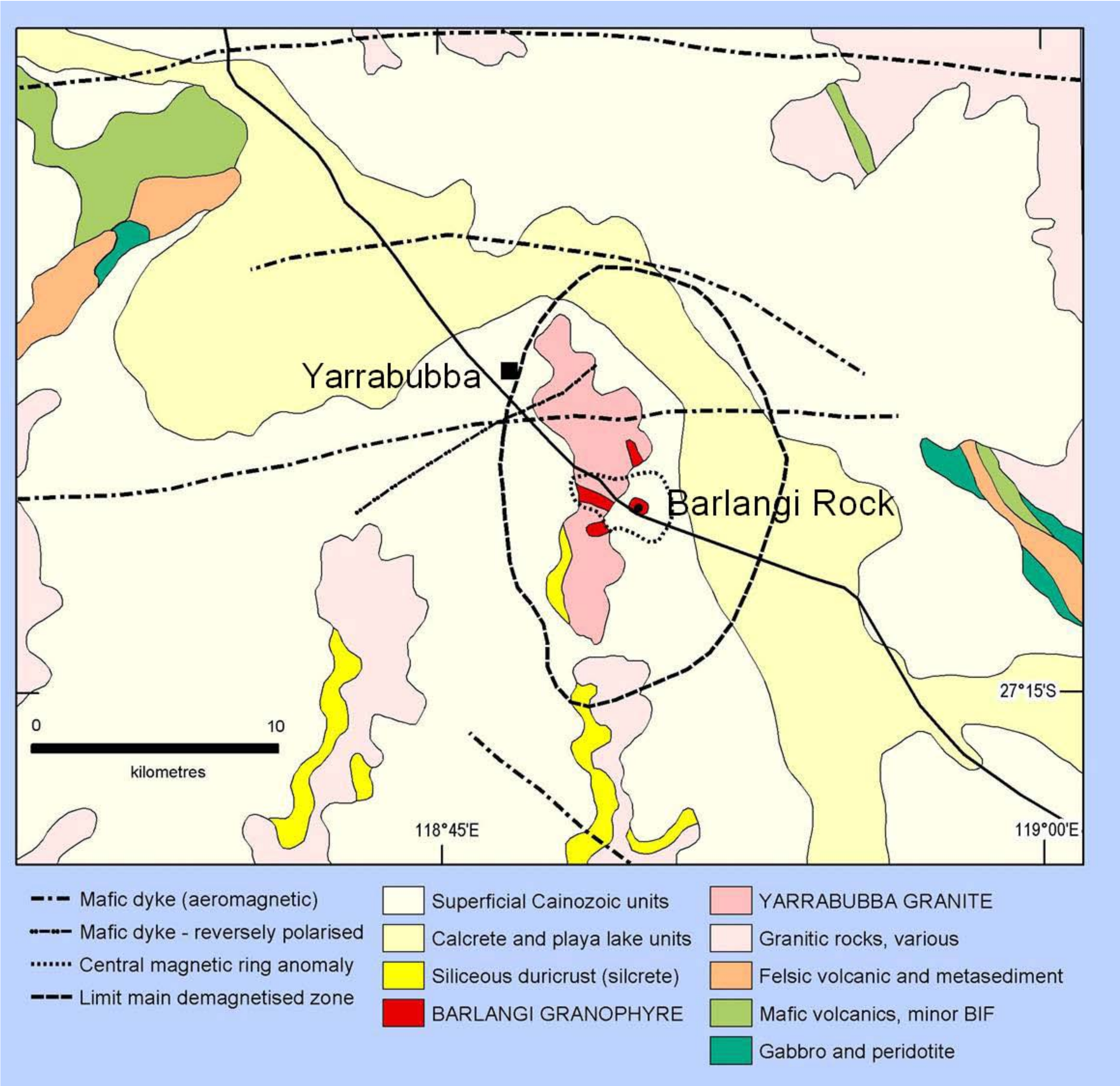

Figure 1: Yarrabubba regional geology.

Yarrabubba Impact Structure

John Bunting

Until recently the only documented impact structures on the Yilgarn Craton were the small Dalgaranga crater, and the Shoemaker Structure (predominantly within the Proterozoic Earaheedy Basin), both of which will be visited on this excursion. The impact record elsewhere indicates that major impact sites should exist on the Yilgarn Craton. The Yarrabubba Impact Structure, first documented by Macdonald et al. (2003) is one such site that gives regional clues to finding others in deeply eroded Archean terranes (Bunting and Macdonald, 2004).

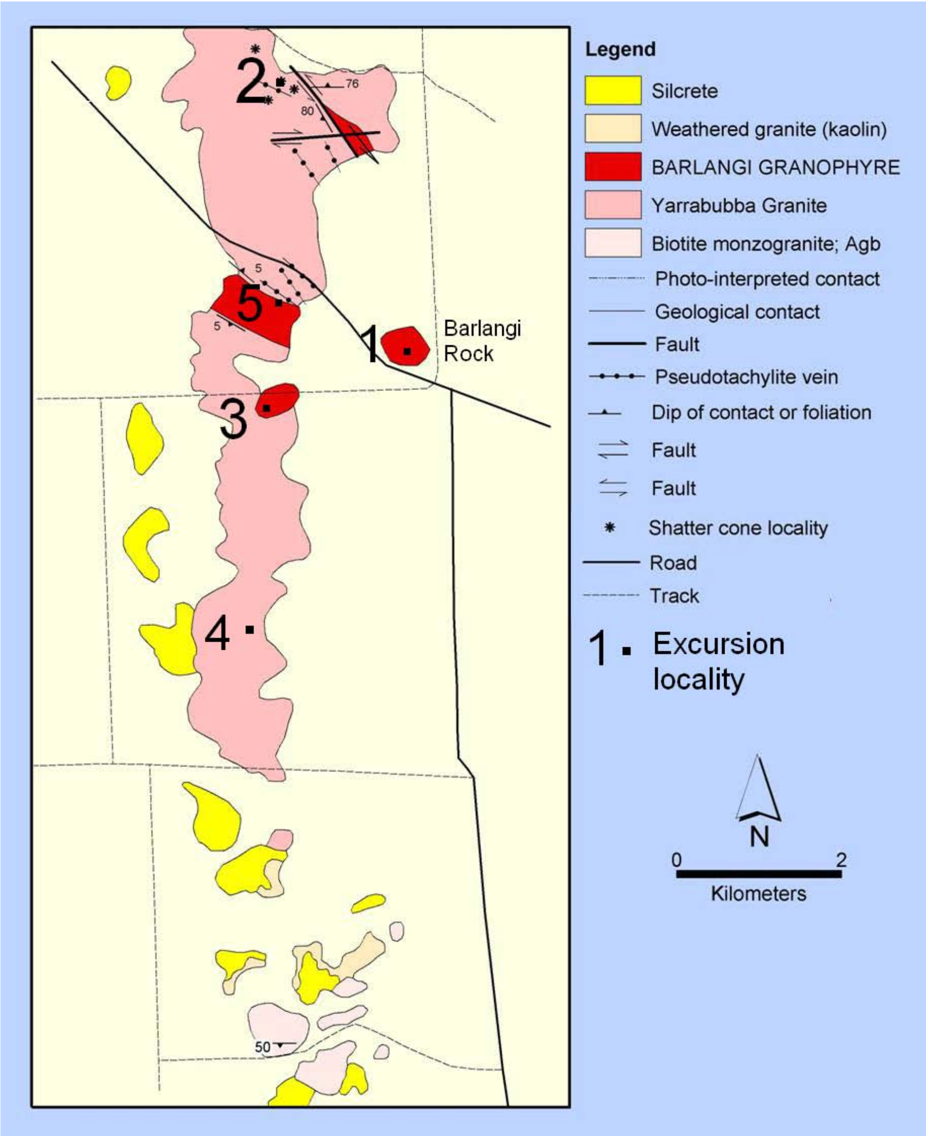

Figure 2: Yarrabubba geology and excursion localities.

The centre of the Yarrabubba Impact Structure (27°11'S 118°50'E) is about 70 km southeast of Meekatharra in the Archean granite-greenstone terrane of the Yilgarn Craton (Figure 1). Unlike most major impact structures Yarrabubba has no obvious circular topographic or geological feature, because it appears to have been eroded to a level well below the crater floor. Outcrop, mainly of granitic rocks, is patchy. Much of the area is covered by superficial alluvium and colluvium, playa lake deposits and valley calcrete. In places deep weathering has kaolinised the granitic rocks and produced a silcrete duricrust. Erosion of the hard silcrete cap and underlying softer kaolinised granite has created spectacular low cliffs ("breakaways") and mesas.

At Yarrabubba, evidence for impact includes shatter cones, planar deformation features (PDFs) in quartz, pseudotachylites and impact breccias, all within the muscovite-bearing Yarrabubba Granite. The centre of the structure is the Barlangi Granophyre, a skeletal-textured felsic rock that is interpreted to have intruded as a multi-lobed sheet of sub-crater impact melt derived from the Yarrabubba Granite (Figure 2).

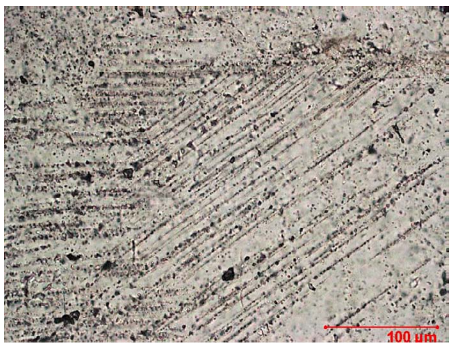

Figure 3: PDFs in quartz, Yarrabubba Granite; GSWA sample 60399 X25 (coll. S Williams, 1979).

Discovery of the impact structure relied on recognition by Steve Williams and Will Libby (Geological Survey of Western Australia) of shock metamorphism in a single thin section (Figure 3) of granite collected in 1979 during regional mapping (Libby, 1979; Tingey, 1985). This was not followed up until the study by Macdonald et al. (2003), who recognised the shatter cones, pseudotachylites, minor breccias, circular magnetic feature and the importance of the Barlangi Granophyre.

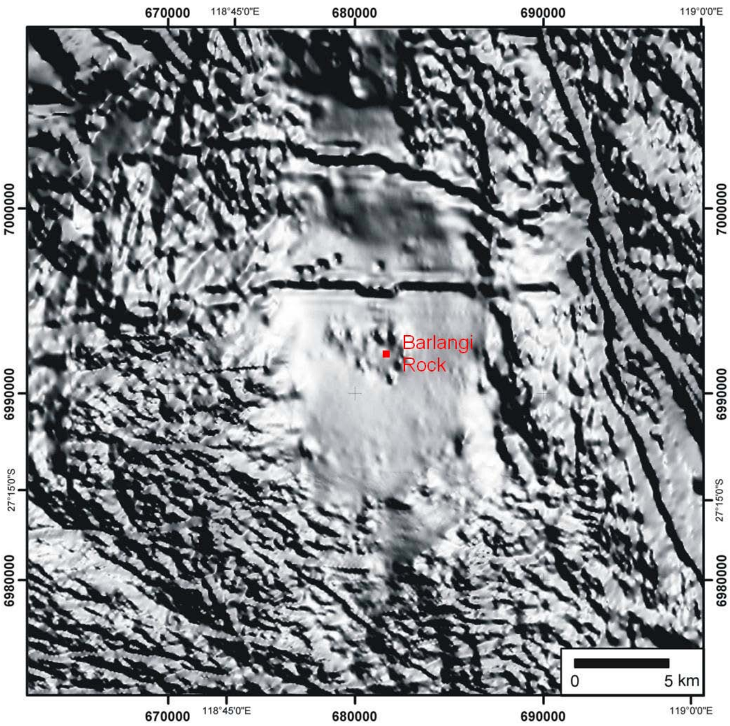

Figure 4: Yarrabubba aeromagnetic TMI image.

The original size of the structure is not known, but some impact effects have been seen in outcrop at least 10 km north (the limit of outcrop) and 9 km south of Barlangi Rock. There is also a 25 x 15 km zone of flat aeromagnetic signature that may represent demagnetisation of the regional granite as a result of the impact (Figure 4). Note the lobate, crudely circular feature in the centre of the demagnetised zone that may have been caused by remagnetisation along the contact of the Barlangi Granophyre with the Yarrabubba Granite.

Three regional features at Yarrabubba are discernable on pre-2002 datasets: (1) the muscovite-bearing Yarrabubba Granite – possibly evidence for alkali metasomatism; (2) the Barlangi Granophyre, distinguished by its unusual skeletal textures; (3) the flat magnetic signature – interpreted as demagnetisation immediately after impact.

The age of the impact is not known with any certainty. Zircons from the Yarrabubba Granite and Barlangi Granophyre give typical Archean ages around 2.6-2.7 Ga (Cassidy et al., 2002; D R Nelson, unpublished data quoted by Pirajno, 2005). The zircons in the Barlangi Granophyre are considered to be xenocrystic, preserved when the granophyre formed by the melting of Yarrabubba Granite during the impact event. Macdonald et al. (2003) concluded on regional grounds that the impact age was probably early Proterozoic. Indirect evidence for an early Proterozoic age is that this northern part of the Yilgarn Craton was probably a peneplaned surface before deposition of the mature sandstones at the base of the Yerrida (>1.9 Ga)and Earaheedy (1.89 Ga, Rasmussen et al., 2012) Groups along the northern margin of the craton. Pirajno (2005) reported an Ar-Ar age of 1134+/-26 from sericitised pseudotachylite, but this could be an alteration age and is therefore a minimum age.

Macdonald et al. (2003) recognised K-metasomatism and reddening of feldspar in the granite. Pirajno (2005) ascribed these, along with veins of bladed calcite and fluorite+biotite/chlorite+prehnite, to hydrothermal alteration associated with the impact.

Excursion localities

Locality 1 is at Barlangi Rock, a prominent rocky hill on the N side of the Meekatharra-Sandstone road at MGA 681770E 6991830N. Park in the trees below the SE side of the hill.

Locality 1: Barlangi Rock

Barlangi Rock is the best of several outcrops of the Barlangi Granophyre. A good route is to climb to the top of the hill, admire the view and the xenoliths, descend the N side, noting the terraces and jointing (Figure 5), then walk east around the base of the hill to the cars.

Figure 5: Terraces of jointed granophyre at Barlangi Rock.

The granophyre is a pink fine-grained rock, with scattered coarser grains of quartz and feldspar, and xenoliths of coarse-grained granite that range from a few centimetres to 0.4 metres across (best seen a few metres north of the summit cairn). Unlike the surrounding Yarrabubba Granite, the granophyre contains no quartz veins, pegmatite, mafic dykes, or pseudotachylite. Gently southwest-dipping terraces are developed on Barlangi Rock (Figure 5), but not in the surrounding granites. Closely spaced fracturing, best seen on the northern side, could be crude columnar jointing related to cooling, or a later (Proterozoic?) regional fabric.

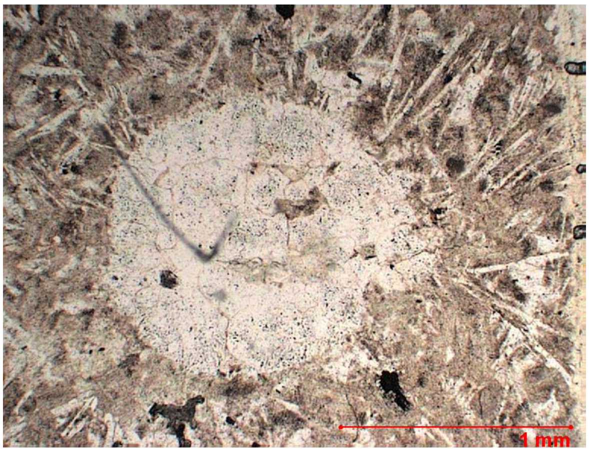

Figure 6: Barlangi Granophyre, Locality 1 – spheroid (xenocryst?) of granulated quartz in groundmass of skeletal-textured quartz and feldspar.

In thin section, the coarser grains in the granophyre appear to be quartz and feldspar xenocrysts. The quartz xenocrysts are rounded, in part resorbed, and consist of a fine mosaic of granulated quartz (Figure 6). Similar granulated textures appear in quartz in the granite xenoliths, in the granite near the granophyre contact, and in the large “pseudotachylite” dykes (see Locality 2b), but not in the regional Yarrabubba Granite. Quartz and clouded feldspar in the Barlangi Granophyre form skeletal textures, indicating rapid quenching (Figure 6). These needles often radiate from quartz xenocrysts, similar to nucleation textures described in the Vredefort (South Africa) impact melt. Shock features (PDFs, shatter cones) have not been observed in the granulated quartz, the granophyre, or the xenoliths.

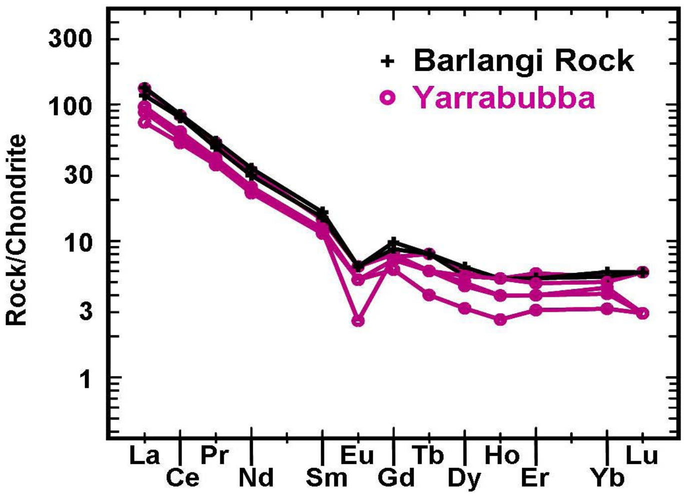

Figure 7: REE plot of five samples of Yarrabubba Granite and two samples of Barlangi Granophyre (data from Cassidy et al., 2002).

The granophyre forms a multi-lobed sheet-like body that is interpreted as an impact-generated melt. Evidence for this includes REE and trace element patterns that are identical to the Yarrabubba Granite and show no evidence for fractionation (Figure 7). Outcrop evidence (see Locality 5), although uncertain, indicates that the contacts of the granophyre are shallow-dipping to horizontal, and the granophyre is overlain and underlain by Yarrabubba Granite. It is possible that the Barlangi Granophyre represents a multi-lobed, sub-crater intrusion of impact-generated melt.

Return to road, turn left, drive 200m and turn left on track. Drive N along W side of fence for 3.7 km to MGA 682045E 6995428N. Turn left on track and drive W for 2.5 km to MGA 680620E 6995563N. Turn left and drive cross-country 250m to Locality 2a at the base of the granite outcrop at MGA 680490E 6995340N.

Figure 8: Shatter cones at Locality 2a.

Locality 2a: Shatter cones and hairline pseudotachylites in Yarrabubba Granite

This is the locality where shatter cones (Figure 8) were first discovered at Yarrabubba in 2002 (Macdonald et al, 2003). The original GSWA thin section, from which PDFs were first described by Will Libby, was from a sample of granite collected by Steve Williams about 1.5 km east of here in 1979.

The Yarrabubba Granite is a pale pink, medium- to coarse-grained monzogranite, consisting of quartz, albitic plagioclase and microcline, with subordinate muscovite and biotite. Here and near Barlangi Rock, quartz grains in the

Yarrabubba Granite display multiple sets of planar deformation features (PDFs) (Figure 3). Plagioclase twin lamellae and cleavages in mica are commonly disrupted or bent. Biotite is commonly altered to a mixture of chlorite and iron oxides, and it also appears that muscovite may have formed from hydrothermal alteration of biotite. Although brecciation in the Yarrabubba Granite is rare, in some outcrops the granite is so highly fractured that it could be classified as monomict breccia.

In general, shatter cones point upwards and have very divergent striation, indicating that the current exposure is far below the original source of the shock wave. Cones range in size from 10cm to, rarely, about 50 cm. Also present, and indeed dominant, are shatter fractures, the diagnostic feature of which is the presence of diverging striated features, known as 'horse-tailing'. Many of the shatter-features at Yarrabubba are best described as shatter surfaces, which are a transitional state between shatter coning and shatter cleavage. Also note sets of curved, discontinuous cleavage.

Figure 9a: Hairline pseudotachylite veins. Note the 10 cm sinistral displacement of a pegmatite vein, top right.

Figure 9b: Detail of left part of Figure 7b, showing "swallowtail" merging of veins.

Also at this locality millimetre-thick black pseudotachylite veins display "cobweb" patterns (Figures 9a and 9b). Note evidence of movement along the veins where pegmatite veins are displaced by a few centimetres. The veins consist of glassy recrystallized granite, which in places, especially in thicker parts where veins join, is a microbreccia (Figure 10). Elsewhere at Yarrabubba (e.g. Locality 5) such black pseudotachylites have been noted up to 20 cm thick.

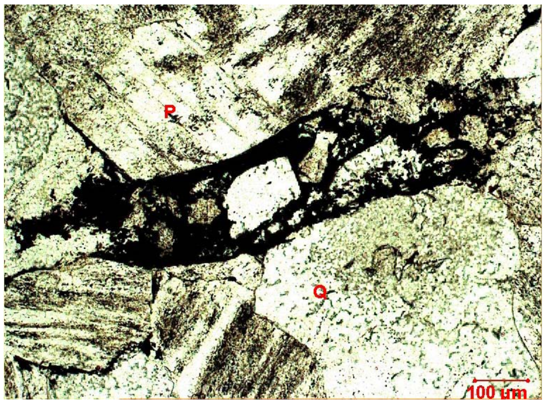

Figure 10 (right): Thin section of microbreccia in pseudotachylite vein (black). P – plagioclase, Q – quartz. Plane-polarised light.

Walk about 230m ESE to Locality 2b at MGA 680684E 6995227N.

Locality 2b: Xenolithic "pseudotachylite" dyke

Within the Yarrabubba structure are numerous dike-like bodies, which range in thickness from a few 10s of centimetres to more than a metre. These bodies are generally of a flinty green aphanitic felsic rock intensely altered (devitrified?) to sericite and quartz, rarely with inclusions of granulated quartz and feldspar. Fault movement is indicated by displacement of pegmatite veins with partially melted pegmatitic clasts strung out within the melt. At Locality 2b the thickest (up to 3m) of these dykes has a central portion containing small (1-2 cm) streaked-out granitic xenoliths with potassium-feldspar

Figure 11: "Pseudotachylite" dyke in Yarrabubba Granite, showing steep south-westerly dip and fracture cleavage.

overgrowths (Figures 11 and 12). Fracture cleavage (partly after flow layering?) and steeply-plunging rodding are also present. In thin section the xenoliths contain resorbed, granulated quartz and hematite-clouded feldspar in a fine-grained quartz-sericite-oxide matrix (Figure 13). Also present in thin section are patches of devitrified glass (Figure 14). These dyke-like bodies are probably fault melts, related to the Barlangi granophyre, injected explosively into the granite.

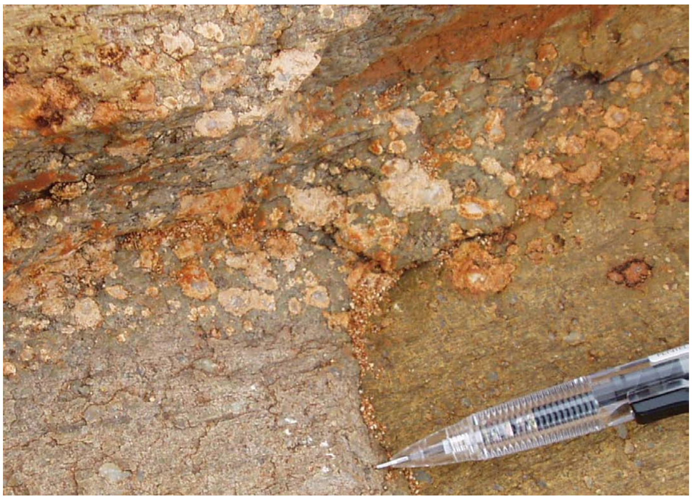

Figure 12: Detail of the central portion of the dyke showing recrystallised rims on resorbed granite-derived quartz and feldspar grains.

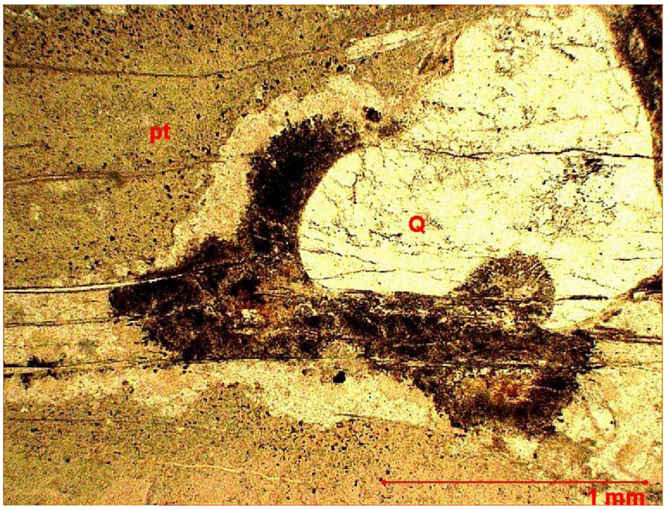

Figure 13 (above): Resorbed and granulated quartz (Q) and iron-stained feldspar (dark) with pink feldspar overgrowth, in "pseudotachylite", with later fractures. Plane-polarised light.

Figure 14 (right): Devitrified glass with flow texture. Plane-polarised light.

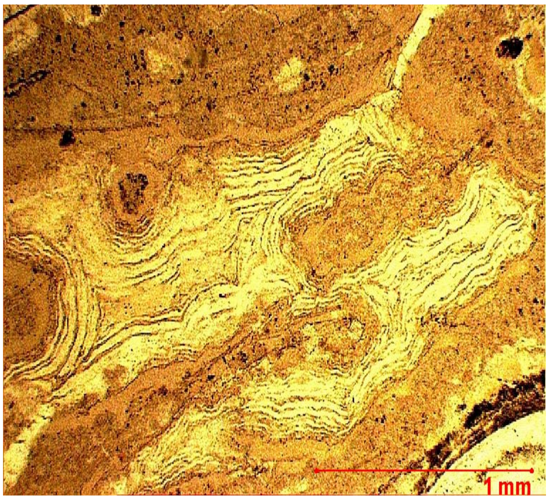

Return to the main road. Turn left, cross the grid, and turn right on the track along the east side of the fence. Follow fence around corner at MGA 681994E 6991616N then west for 1.9 km. Walk S 100m to Locality 3a at MGA 680110E 6991480N.

Locality 3a: Quarry locality – Barlangi Granophyre

The Barlangi Granophyre at this locality is very fresh. As at Barlangi Rock (Locality 1) the granophyre contains small granite xenoliths (Figure 15) and resorbed xenocrysts of quartz and feldspar. The low outcrops of granophyre show a faint layering on the weathered surface. The layering has generally steep dips, with the strike varying between NNW and NE. One outcrop shows the layering wrapping around a 10 cm granite xenolith. This is one of the two sampling sites of Barlangi Granophyre described by Cassidy et al (2002). The REE profile is shown in Figure 7.

Outcrops and many of the loose fragments around the outcrops have been reworked, possibly by Aborigines. Please do not disturb or remove this material.

Figure 15: Granite xenoliths in Barlangi granophyre. Scale is 10cm across.

Walk about 200m to the SE side of the clearing, just beyond the last scree of granophyre, to some granite boulders at MGA 680270E 6991380N.

Locality 3b: Quarry locality – Yarrabubba Granite

This is one of the five sample sites of Yarrabubba Granite described by Cassidy et al (2002). At the blast site the fresh coarse-grained monzogranite contains altered alkali feldspar, its brick-red colour caused by Fe-oxide dusting, and pale green-grey sericitised plagioclase. Dark-grey fine-grained pseudotachylite is present as a vein 2-3 cm wide and as several thinner veins and irregular patches. The granite outcrop is very close to the contact with the granophyre. This contact coincides with the lobate, circular magnetic feature at the centre of the large demagnetized zone on the aeromagnetic map (Figure 4).

From the fence N of Locality 3a, drive S through the scrub for 2.8 km to Locality 4 at MGA 679670E 6988810N. Note: Because of time constraints and difficult access it might not be possible to visit Locality 4 on this excursion.

Locality 4: Impact breccia

This is the only locality at Yarrabubba where an impact breccia has been found (illustrating the amount of erosion of the original crater). Outcrop is poor and consists mainly of scattered rubble of slightly weathered Yarrabubba Granite. The impact breccia consists of a few blocks 20-30 cm wide, suggesting a narrow dyke-like form. The breccia is pale pink/cream with irregular angular fragments up to 2 cm across (Figure 14). Although some fragments are granitic some are of a fine-grained felsic rock of uncertain origin. Also puzzling are small fragments of deformed mafic material.

Figure 16: Hand specimen of impact breccia showing granitic fragments (e.g. bottom left) and deformed mafic fragments (dark). Note the vertical pseudotachylite vein near right edge. The orange-brown parts are surface weathering.

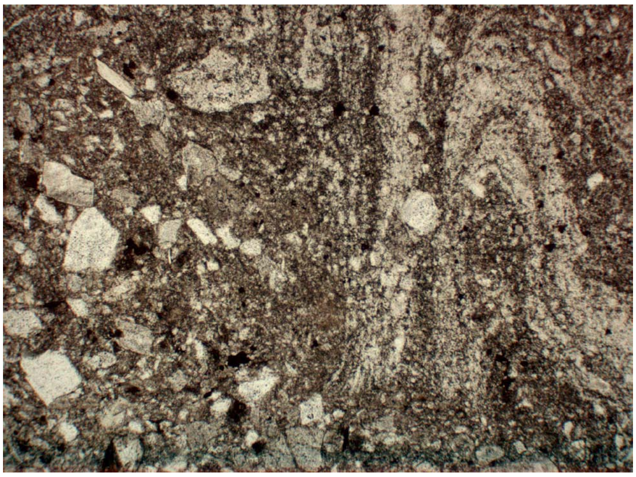

Figure 17: Microbreccia showing folded flow banding. Plane-polarised light. Field of view: 2.9mm across.

In thin section (Figures 17, 18a and 18b) the groundmass is shown to be angular fragments, about 1 mm across, of deformed quartz, feldspar (including microcline and albite) and muscovite, set in a finer matrix with a grain size <0.1 mm. Some folding may represent fluidization of the matrix (Figure 17).

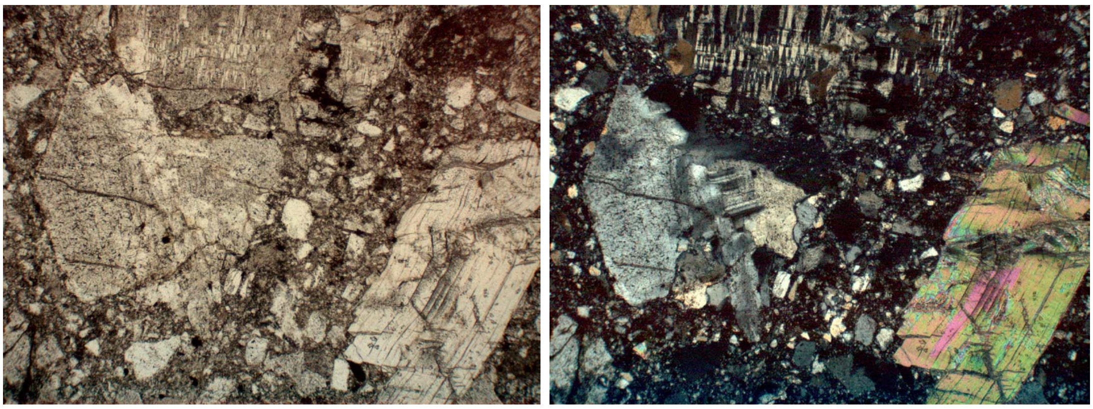

Figure 18a (left): Coarse granite (left centre), microcline (top) and muscovite fragments in microbreccia. Plane-polarised light.

Figure 18b (right): Same view as 16a. Crossed Nicols.

Field of view is about 2.9mm across.

Return the 2.8 km N to the E-W fence, turn right and return to the main road. Turn left and drive for about 2.0 km to park on the left side of the road near MGA 680450E 6993060N. Locality 5 is a traverse from here up the hill to the SW.

Locality 5: Granophyre contact

Before walking up the hill to the south, inspect the Yarrabubba Granite immediately north and south of the road. There are some weak crescentic shatter surfaces, a pale green sericitised "pseudotachylite" dyke, and remobilised quartz veins.

Walk southwest over the granite outcrops and up the low hill, about 400 metres. On the way look for remobilised quartz veins, fractured (almost brecciated) granitic pegmatite, and more of the pale green "pseudotachylite" dykes.

At Locality 5 MGA 680190E 6992740N we are on the contact between the Yarrabubba Granite to the NE and a lobe of Barlangi Granophyre to the SW. The quartz in the granite has a distinctive sugary texture – the result of granulation of the original coarse grains. The slightly weathered granophyre is similar to that on Barlangi Rock. The contact can be followed to the NW for about a kilometre. In places the actual contact is exposed or nearly so, and it appears (inconclusively) that the contact dips at a low angle to the NE i.e. the granite overlies the granophyre. Locally the complex shape of the contact again suggests a very shallow dip. The granophyre can be traced for about 600m across strike. The SW contact against granite is less well exposed, but again can be traced for a kilometre or so.

Close to the northern granite-granophyre contact there are numerous scree fragments of black pseudotachylite. The rock is similar to the black veins at Locality 3b, but coarser grained. Relict patches of granulated quartz, rimmed by red feldspar similar to the dyke at Locality 2b, are set in a dark siliceous micro-brecciated matrix that contains some faint skeletal texture. The size of the scree fragments suggests that they originated in veins or small dykes up to 20 cm wide. None has been found in outcrop. Given that the black pseudotachylite is very hard and resistant it is possible that the scree fragments represent a lag deposit of veins long since removed by erosion.

Return to the main road. This ends the Yarrabubba part of the excursion. Drive NW to Meekatharra, about 90 km.

References

Bunting, J. A. and Macdonald, F. A., 2004. The Yarrabubba Structure, Western Australia – clues to identifying impact events in deeply eroded ancient cratons. 17th Australian Geological Convention, Hobart, February 2004 Abstracts Volume (Geological Society of Australia, Abstracts v73), p 227.

Cassidy, K. F., Champion, D. C., McNaughton, N. J., Fletcher, I. R., Whitaker, A. J., Bastrakova, I. V. and Budd, A. R., 2002. Characterisation and metallogenic significance of Archaean granitoids of the Yilgarn Craton. Minerals and Energy Research Institute of Western Australia, Report 222.

Libby, W. G., 1979, Petrography of 35 rocks from the Sandstone 1:250,000 Sheet: Geological Survey of Western Australia, Petrology Report No. 1007 (unpublished).

Macdonald, F. A., Bunting, J. A. and Cina, S. E., 2003. Yarrabubba – a large deeply eroded impact structure in the Yilgarn Craton, Western Australia. Earth and Planetary Science Letters, 213, p. 235-247.

Pirajno, F., 2005. Hydrothermal processes associated with meteorite impact structures: evidence from three Australian examples and implications for economic resources. Australian Journal of Earth Sciences, 52, p. 587-605.

Rasmussen, B., Fletcher, I.R., Bekker, A., Muhling, J. R., Gregory, C. J. and Thorne, A. M., 2012. Deposition of 1.88-billion-year-old iron formations as a consequence of rapid crustal growth. Nature, 484, p. 498-501.

Tingey, R. J., 1985. Sandstone, WA. Geological Survey of Western Australia, 1:250,000 Geological Series, Explanatory Notes.

Notes

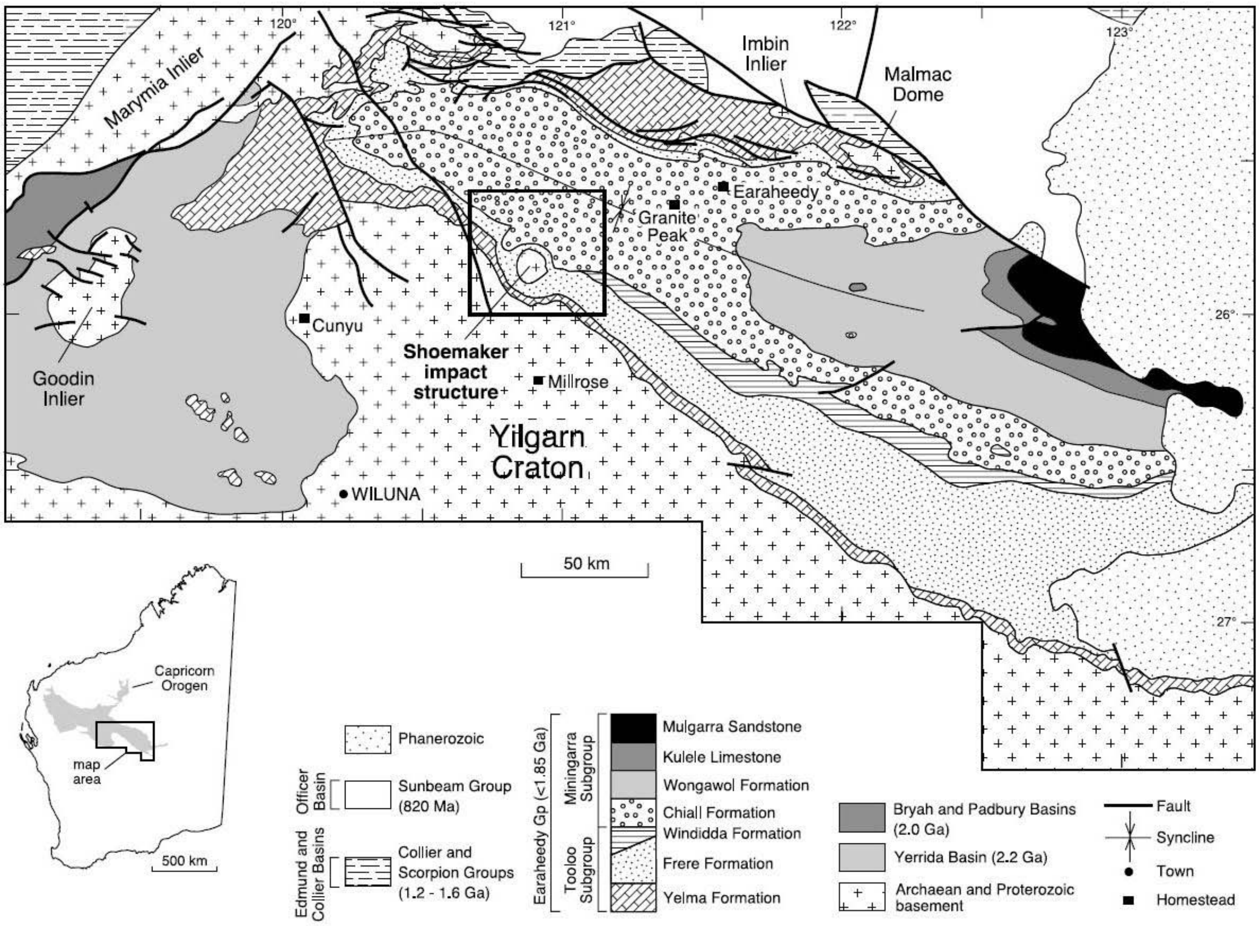

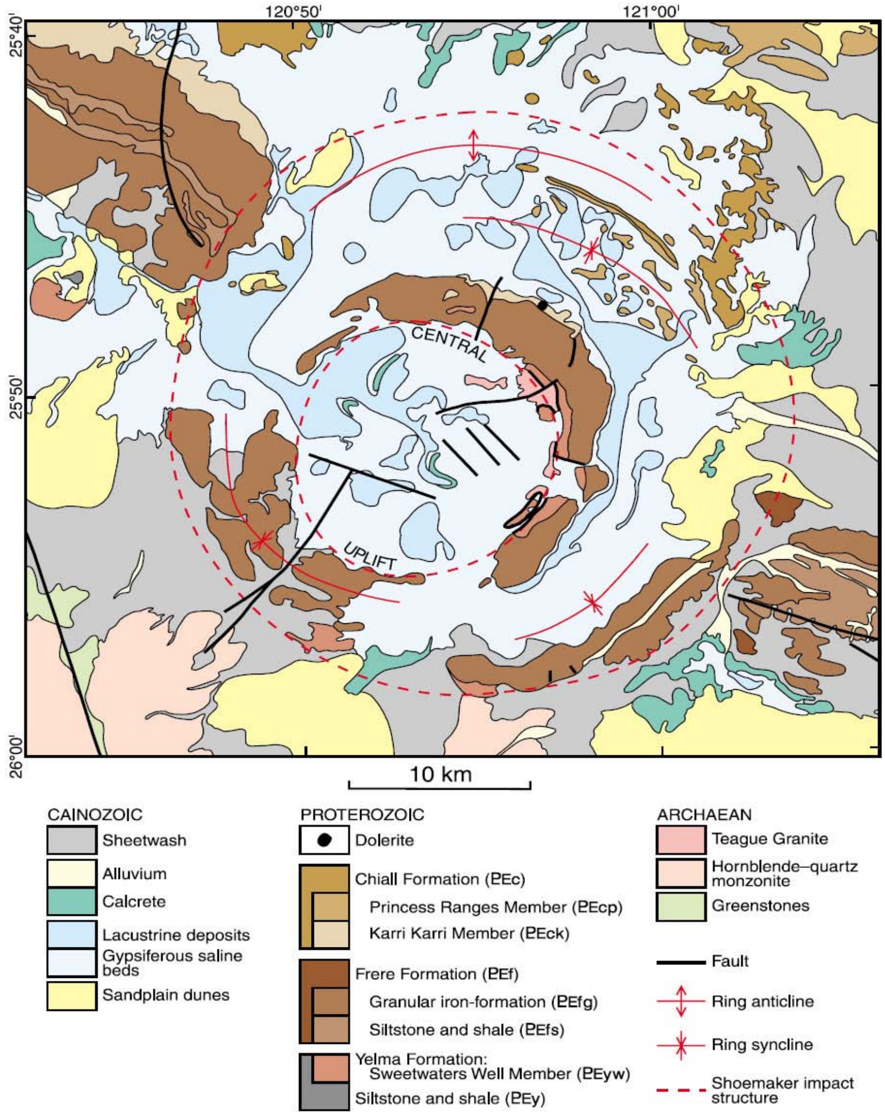

Figure 1a (above): Simplified geological map of the Earaheedy Basin on the northern margin of the Yilgarn Craton. Square shows location of Figure 2.

Figure 1b (left): Simplified geological map of the Shoemaker Impact Structure.

Both figures are from Pirajno et al. (2003).

Shoemaker Impact Structure John Bunting and Mike Freeman

The Geological Survey of Western Australia has supplied each delegate with a copy of the Geological Survey of Western Australia Report 82 by Franco Pirajno, detailing the geology of the structure and including his mapping dated from 2002. Consequently the following general description is brief.

The Shoemaker Impact Structure (SIS) is located at 25°52'S, 120°53'E, about 100 km northeast of Wiluna, and 850 km north-northeast of Perth (Figure 1a). The structure is at the southern edge of the Paleoproterozoic Earaheedy Basin close to the exposed northern margin of the Archean Yilgarn Craton. It consists of a central core, about 12 km across, of predominantly granitic rocks, surrounded by a complex ring syncline about 20-25 km across in Paleoproterozoic sedimentary rocks (Figure 1b).

The structure interrupts prominent lines of hills of the northwest-trending Frere Range, which rise about 50 – 70 m above the surrounding plain. Two concentric rings of low hills, formed by iron-rich sedimentary rocks of the Frere Formation, define the shape of the structure. Ephemeral playas of Lake Nabberu, Lake Teague, and Lake Shoemaker occupy the poorly exposed areas between the two rings and in the area of the central uplift (Figure 2, and see also the front cover of this guide).

The SIS was first described by Butler (1974), who named it the Lake Teague ring structure. He suggested it might have formed as either the result of granite intrusion or an impact event. Bunting et al (1980, 1982) carried out systematic mapping in the area and described evidence for shock metamorphism, including shatter cones and planar deformation fabrics (PDF) in quartz. On geological grounds they concluded that the structure was caused by a cryptoexplosive event that was non-random and therefore may not have been caused by a meteorite impact. During 1986 and again in 1995 Eugene and Carolyn Shoemaker conducted fieldwork and confirmed the presence of shock metamorphism, concluding that the structure was formed by extraterrestrial impact (Shoemaker and Shoemaker, 1996). Sadly, Eugene died in a car accident on 18th July 1997 during a geological field trip that had included another visit to SIS. In commemoration of his life and contribution to astrogeology, the Lake Teague ring structure was renamed the Shoemaker Impact Structure (Pirajno and Glikson 1998). Pirajno (2002, 2005) and Pirajno et al. (2003, 2004) reported detailed investigations of the structure, following 1:100,000-scale mapping by the Geological Survey of Western Australia (Pirajno, 1998).

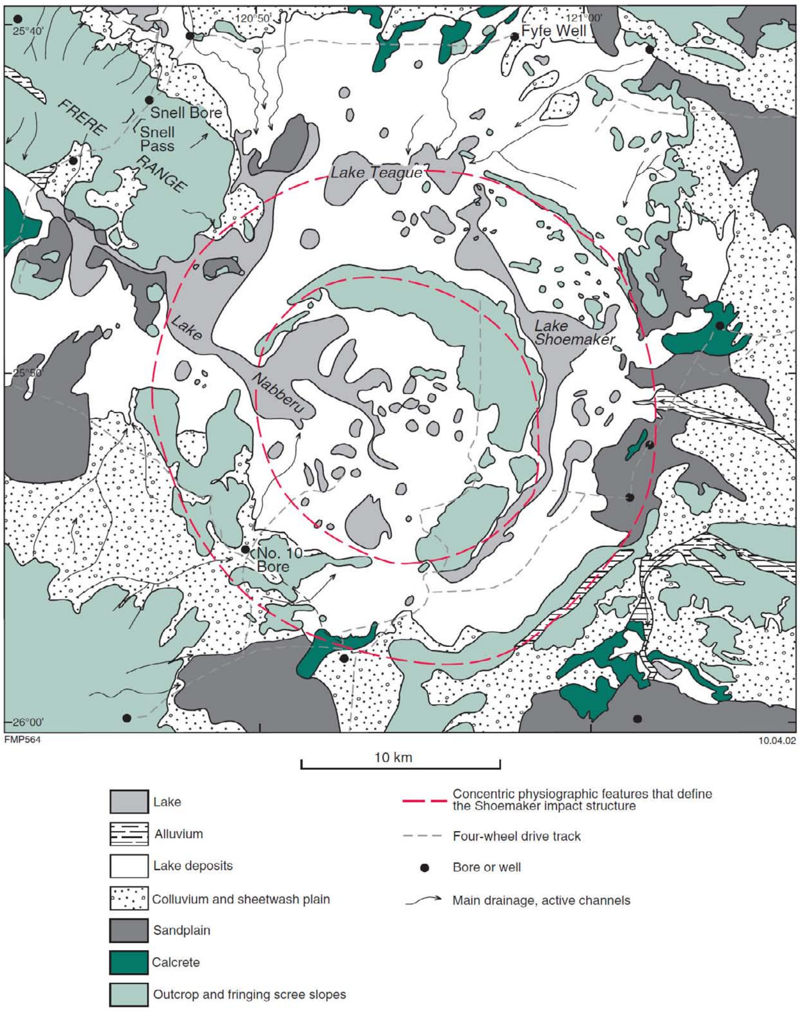

Figure 2: Physiographic map of the area around the Shoemaker impact structure. From Pirajno (2002).

The Shoemaker Impact Structure is a deeply eroded structure. Pirajno (2002) suggests that 2-3 km of overlying rock may have been removed by erosion. Estimates for the original crater diameter range from 36 to 90 km, depending on how it is defined (Glikson, 2002). The structure has been formally assigned a diameter of 30 km, which corresponds to its visible extent. The structure is asymmetrical, with an apparent tilt to the northeast, probably by post-Earaheedy Group but pre-impact tectonism. Pirajno (2002, 2005) notes an east-west asymmetry in the higher magnetic intensity and hydrothermal alteration on the eastern side of the central uplift.

Regional setting

The pre-impact regional geology involves two principal components: the Archean granite-greenstone terrane of the Yilgarn Craton and the Paleoproterozoic sedimentary sequence of the Earaheedy Basin (Earaheedy Group).

Dolerite, possibly a sill, outcrops on the northeast inner rim of the SIS. The emplacement age of the dolerite is not known, but the most likely affiliation is with the numerous dolerite sills of the 1.07 Ga Warakurna Large Igneous Province (Wingate et al., 2004), numerous examples of which intruded the Mesoproterozoic Bangemall Superbasin some 100 km north and northeast of the SIS. Aeromagnetic data show several linear features that are almost certainly mafic dykes. Pirajno et al. (2004) suggest that the sill and dykes post-date the impact.

Yilgarn Craton

Archean greenstones are exposed in a NNW-trending belt about 30 km southwest of the centre of the SIS. Evidence from geophysical interpretation and exploration drilling suggests that greenstones unconformably underlie the Earaheedy Group along the southwest and southeast margins of the SIS. The main rock types are metamorphosed mafic and felsic volcanic rocks, with minor metasedimentary and ultramafic rocks. The greenstones form part of the Laverton Domain of the Kurnalpi Terrane of the eastern Yilgarn (Cassidy et al., 2006). The major mafic-felsic magmatic event in the Laverton Domain has been dated at around 2.81Ga. The central uplift of the SIS contains outcropping remnants of schistose mafic/felsic/sedimentary rocks within the Teague Granite, and Pirajno (2002) interprets an unexposed NW-trending greenstone wedge in the southern part of the Teague Granite.

Granite in the Kurnalpi Terrane is mainly biotite monzogranite and syenogranite ranging in age from 2.7-2.65 Ga. Granite south and southwest of the SIS is mostly hornblende quartz monzonite and hornblende monzogranite. It is coarse grained, consisting of orthoclase, microcline, oligoclase, quartz and dark green euhedral hornblende, with minor biotite, epidote and titanite. Nelson (1999) determined a SHRIMP U-Pb age of 2664 Ma for the hornblende quartz monzonite. Archean granite, including alkaline leucogranite and pyroxene-bearing quartz syenite, collectively termed the Teague Granite, is present in the central core of the SIS, but it been considerably modified by the impact (see below).

The greenstone belt to the southwest of the SIS, near Horse Well, contains some small historical gold workings and some uneconomic gold resources (<100,000 ounces), mainly in shear-hosted veins. Elsewhere the Laverton Domain has significant deposits of gold, nickel, copper-zinc and rare-earth elements.

Earaheedy Group

Subgroup	*Formation*	*Lithology*	*Thickness*	*Comments*
Miningarra Subgroup	Chiall Formation	Siltstone, shale, with glauconitic sandstone and mature quartzite beds in the upper part.	100+ m	In the SIS area, only present in the northeast part of the rim syncline. Not visited on the excursion.
Tooloo Subgroup	Windidda Formation	Shale, mudstone and stromatolitic limestone.	0-300? m	Only present east of the SIS. May be unexposed in eastern rim syncline.
	Frere Formation	Granular iron-formation, shale, ferruginous chert, BIF, dolomite.	600 m	Mainly GIF and shale at SIS. Locally Fe and Mn rich.
	Yelma Formation	Basal sandstone/conglomerate, shale, stromatolitic dolomite.	20-300? m	Limestone commonly silicified (in and outside the SIS). MVT deposits.

Table 1: Stratigraphy of the Earaheedy Group in the area of the Shoemaker impact structure.

The Earaheedy Group, which sits unconformably on the Yilgarn Craton at Shoemaker, occupies the Earaheedy Basin and is a thick package of shallow-marine clastic and chemical sedimentary rocks. In total it is about 5000 metres thick, but only the lower three formations (the Yelma, Frere and Chiall Formations) are involved at the SIS (although a carbonate/shale unit, the Windidda Formation, has been mapped between the Frere and overlying Chiall Formations to the east of the SIS). A summary of the formations is given in Table 1.

Figure 3: Ironstones of the Frere Formation.

The Earaheedy Group was deformed by the Capricorn Orogeny (~1.8 Ga), which created a gentle northeast tilt in the southern part of the basin, but intense folding, faulting and cleavage in the northern part. Good recent summaries of the Earaheedy Group and its tectonic setting in the Capricorn Orogen are given by Pirajno et al. (2009) and Muhling et al. (2012).

Until recently the maximum depositional age of the Earaheedy Group was poorly constrained by dating of detrital zircons between 2.0 Ga in the lowermost part of the sequence and 1.8 Ga near the top (Nelson, 1997; Pirajno et al., 2009). Rasmussen et al. (2012) have now dated volcanic zircons from tuff beds in a drill hole in the basal Frere Formation about 40 km northwest of the SIS. The SHRIMP Pb-Pb data give a depositional age of 1.89 Ga for the basal Frere Formation. Muhling et al. (2012) reported minimum depositional ages from the underlying Yelma Formation. Authigenic monazite intergrown with primary sulphide minerals gave a SHRIMP Pb-Pb age of about 1.81 Ga, and xenotime outgrowths on detrital zircon an age of about 1.83 Ga.

Description of the impact structure

The two components that define the Shoemaker Impact Structure are the concentric ring syncline/anticline structures, formed mainly in Frere and Chiall Formations, and the central core of Archean, mainly granitic rocks (Bunting et al, 1980; Pirajno, 2002).

The ring structures consist of an outer ring anticline and an inner ring syncline. Because of the asymmetry of the structure the folds on the northeast side are much wider, and it is here that the main ring syncline contains shale and sandstone of the Chiall Formation. The outboard ring anticline is absent from the southwest side of the structure. There is a complex pattern of faults, some of which contain quartz veins. In the eastern portions, thrusting and shearing introduce additional complexity. Outside the structure, radial quartz veins appear to converge towards the centre.

Figure 4: Teague Granite in the centre of the structure.

The central core (Figure 4) contains various granite types, principally syenite, quartz syenite and leucocratic granite (Bunting et al., 1980; Johnson, 1991; Pirajno, 2002), collectively named the Teague Granite (Pirajno, 1998). These have been uplifted relative to the enclosing Earaheedy Group and are now considered to be within the central uplift of the impact structure. The following descriptions are from Pirajno (2002; 2005).

The syenite is medium grained, pink to brick red, and contains about 55% orthoclase phenocrysts and 15% zoned alkali pyroxene (sodic hedenbergite or aegirine augite), with 25% albite in the groundmass. Accessories include green fibrous amphibole, zircon and andradite garnet. The quartz syenite is similar to the syenite in grain size and colour but has a polygonal and granoblastic texture. Albite and quartz, in roughly equal proportions, are overprinted by perthitic microcline. Accessories include alkali pyroxene, amphibole, zircon and titanite. The leucocratic granite consists of quartz and microcline, +/- albite, biotite and sericite. Unlike the syenitic rocks the texture of the leucocratic granite is distinctly cataclastic.

Pirajno (2002, 2005) concluded that the various rock types in the Teague Granite, along with alteration assemblages and veins in remnants of greenstones, resulted from deformation, alkali metasomatism and hydrothermal alteration of Archean rocks by the impact. A possible candidate for the pre-impact precursor of the pyroxene-bearing alkaline rocks is the hornblende quartz monzonite outside the SIS.

Age

The age of the Shoemaker Impact Structure is poorly constrained, largely because the rocks have undergone a complex sequence of thermal events over time. The impact must post-date deposition of the Earaheedy Group, and a recently reported Pb-Pb (SHRIMP) age of 1.88 Ga on volcanic zircon from the Frere Formation therefore gives a maximum age of the impact (Rasmussen et al., 2012). A number of different dating methods have been used on samples of the Teague Granite, and these provide widely varying ages. SHRIMP U-Pb dating of zircons extracted from the granite returned 2648 ± 8 Ma, which is interpreted to be the magmatic age of the granite (Nelson, 1997). Rb-Sr dating on whole-rock granite samples returned ages of 1630 and 1260 Ma (Bunting et al., 1980), which are now interpreted to be ‘resetting’ by thermal events at 1630 Ma and intense weathering at 1260 Ma (Pirajno and Glikson, 1998; Pirajno et al., 2003). Ar-Ar dating returned disturbed apparent ages of about 1300 and1000 Ma, the latter age possibly being related to the emplacement of a dolerite sill on the northern edge of the inner ring at about 1070 Ma. K-Ar analyses on clay minerals from the granite provided ages of 694 ± 25 and 568 ± 20Ma.

The K-Ar technique has previously been successful at determining the tectonic and thermal histories of sedimentary basins, and Pirajno (2002, 2005) therefore takes 568 Ma as the most likely age of the impact; however the two K-Ar ages are inconsistent, and there is no certainty that the clay minerals sampled were the direct result of processes associated with the impact. Pirajno et al. (2004) describe the dolerite in the northeast inner ring as undeformed and possibly post-impact. If this is correct, and if the dolerite is part of the 1.07 Ga Warakurna Large Igneous Province, then a late Paleoproterozoic to early Mesoproterozoic age of impact is more likely.

Evidence for impact

Circular structure:

The most striking feature of the Shoemaker Impact Structure is the two concentric rings of iron-rich rocks, which mark a well-defined circular structure around a 12 km diameter core of Archean granitic rocks (Figures 1, 2 and front cover of this guide). There is evidence of uplift of the granitic core accompanied by faulting and generation of ring syncline and anticline.

Shatter cones:

Shatter cones up to 30 cm long occur in the granular iron-formation of the Frere Formation (Bunting et al., 1980; Pirajno, 2002). Sandstone of the Chiall Formation contains shatter cones up to 0.5 m in length about 15 km northeast of the centre of the SIS (Figure 5), and poorly developed shatter cones have been described from silicified carbonate rocks of the Yelma Formation immediately east of the central uplift (Pirajno, 2002). With the eye of faith, shatter cones can be identified in the Teague Granite.

Figure 5: Shatter cones in the Chiall Formation.

PDFs:

Planar deformation features, mainly of the decorated variety defined by lines of fluid inclusions, are present in quartz in the leucocratic portion of the Teague Granite (Figure 6) (Bunting et al., 1980; Pirajno, 2002). They appear to be absent (or rare?) in the syenitic phases.

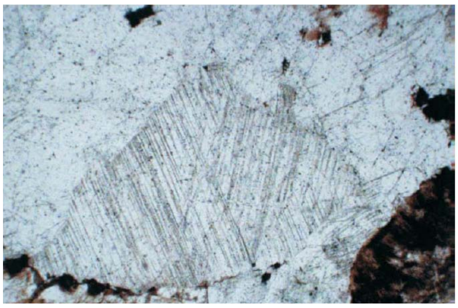

Figure 6: PDFs in quartz of Teague Granite. From Pirajno (2002)

Planar fractures:

Planar fractures are found in quartz grains of Chiall Formation sandstone, near the location of the shatter cones.

Pseudotachylite veins:

Bunting et al. (1980) describe narrow (<1mm) pseudotachylite veins, consisting of quartz and feldspar fragments in a devitrified glassy matrix, in the granite and syenite. (e.g. Figure 7). In the same thin sections plagioclase crystals are shattered and twin lamellae disrupted.

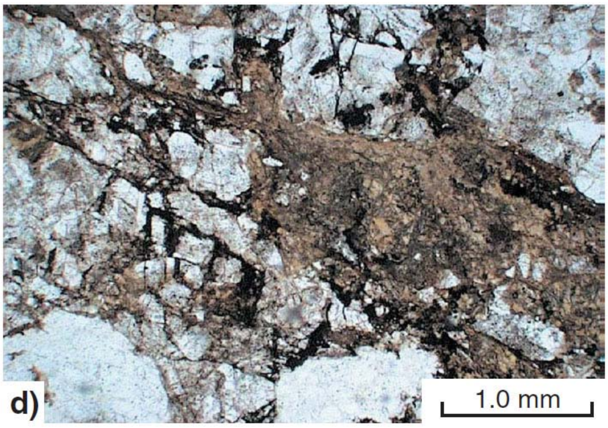

Figure 7: Pseudotachylite veinlets cutting across an albite–quartz assemblage and infilled with sericite Plane-polarized light. From Pirajno (2002).

Fracturing and brecciation:

Much of the granitic rock in the central core is intensely fractured. About 15 km NNE of the centre of the SIS is a lag deposit of centimetre- to metre-sized rounded and angular boulders of sandstone. Pirajno (2002) suggests that the fragments represent reworked lithic breccia ejecta or crater-fill allochtonous breccia, although Bunting et al. (1982) considered them to be a lag deposit from Permian glacial rocks.

Geophysical signatures:

Pirajno (2002) describes gravity lows and demagnetized aeromagnetic patterns that are consistent with similar patterns from other impact structures. He suggests that an inner circular magnetic high along the eastern side of the core could be enhanced magnetic susceptibility caused by hydrothermal alteration of hematite to magnetite after impact.

Metasomatism and hydrothermal alteration:

Pirajno (2002, 2005) ascribes numerous features of the SIS to impact-related metasomatism and hydrothermal alteration, including sodic pyroxene, potassium enrichment of feldspar, and silicification in the Teague Granite.

Excursion localities (Figure 8)

Because of the scale of the SIS and difficulties of access (such as playa lakes and poor tracks) the excursion will concentrate on the exposed eastern core, adjacent parts of the inner ring, and the iron formations along the northern inner ring. Access is via Millrose homestead and station tracks to Billabong Bore (MGA 287500E 7126700N), thence NE along a moderately good track for about 13 km to Locality 1 at MGA 293735E 7135257N.

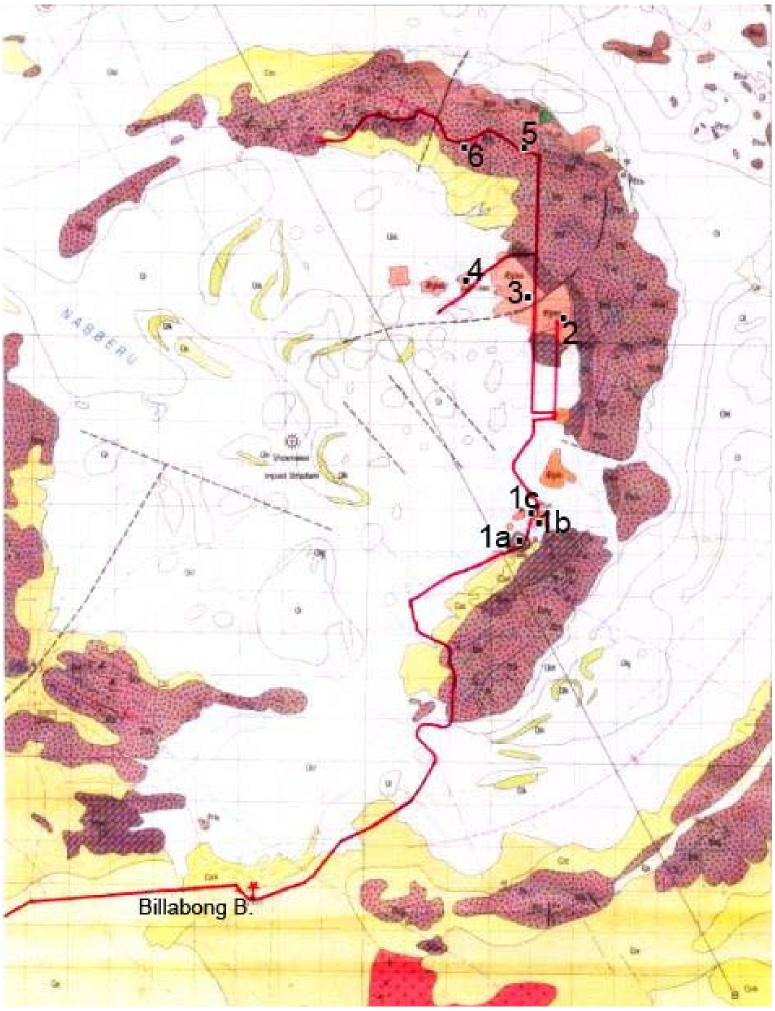

Figure 8: Excursion localities. For geology, see Figure 1. Base map from Pirajno (1998). Grid squares are 1 km.

Locality 1a: Leucogranite, silicified stromatolites and mineralization

Outcrop near the track is leucogranite of the Teague Granite. The composition is quartz, plagioclase, pale pink alkali feldspar and rare biotite. The texture looks recrystallized, and there is closely spaced fracturing – both probably related to the impact event.

Figure 9: Stromatolites (*Asperia digitata*) in silicified dolomite of the Yelma Formation.

To the west there is poorly outcropping chert (silicified carbonate) of the Yelma Formation. The chert has a wavy lamination with well-preserved stromatolites of the form *Asperia digitata* (formerly *Yelma digitata*) (Figure 9) – a form characteristic of the dolomitic Sweetwaters Well Member of the Yelma Formation (Grey, 1984, 1994). Silicification of carbonate is common in the Yelma Formation throughout the Earaheedy Basin, although here it is particularly severe. Rare float of chert breccia has a sulphurous smell and oxidised material that may be oxidised base-metal sulphides. However preliminary analysis using a Niton portable XRF indicates no anomalous base metals. The rock is essentially silica (analysis courtesy of Don Boyer). Base metal mineralization is common in the Sweetwaters Well Member near the top of the Yelma Formation. At Sweetwaters Well, 60 km northwest of Locality 1, fresh galena is present in outcropping stromatolitic dolomite (Bunting, 1986). Exploration drilling of the Sweetwaters Well Member, mainly by Renison Goldfields Consolidated, defined several prospects with zinc, lead and copper sulphides in Mississippi Valley-type (MVT) mineralization (Pirano et al, 2004).

Walk/drive 600m northeast along the track, then to a low outcrop about 100m southeast of the track.

Locality 1b: Quartz arenite – Yelma Formation?

This outcrop of mature, fine- to medium-grained quartz arenite is presumably Yelma Formation; however it is somewhat enigmatic. The rock type, shallow-marine features and stratigraphic position are typical Yelma, but there is no evidence of the deformation that we would expect within the central uplift of a major impact structure. Petrological examination might show evidence of shock effects (e.g. PDFs). If there are none, then it is possible, if unlikely, that the shock waves concentrated in zones of weakness that bypassed this locality. Alternatively, is this evidence of a post-impact, transgressive, shallow-marine sequence that flooded the crater?

Walk/drive about 500m along the track to a low outcrop at MGA 294090E 7136040N.

Locality 1c: Granite, greenstone and Yelma Formation

Near the track is outcropping leucogranite of the Teague Granite. The granite is pervasively shattered and fractured. About 40m to the west poorly exposed mafic schist, with a WNW-trending vertical foliation, is probably a selvage of metamorphosed Archean greenstone caught up in the granite.

To the west, about another 100m, a narrow outcrop of immature sandstone strikes north-northeast, with a shallow easterly dip. The sandstone may originally have been glauconitic, another typical feature of the Yelma Formation. The eastern contact with the granite is probably a fault, but at the western contact the sandstone could be unconformable on the granite. The sandstone can be followed for at least 300m to the southwest where it thickens and contains poorly exposed beds of carbonate (probably originally dolomite, but now largely secondary calcrete). The sandstone, especially on the eastern side of the outcrop, is severely shattered.

Drive north for about 2.4 km to a fence, turn right and after 600m turn left and follow the track on the east side of the fence north for about 2.4 km to a small creek at MGA 294600E 7140500N. [If time is short Locality 2 might be omitted or visited later in the excursion.]

Locality 2: Shattering in leucocratic Teague Granite

Walk northeast along a small creek. The leucocratic variant of the Teague Granite is fractured and shattered by the impact. At MGA 294705E 7140585N the shattering is intense, and includes some possibly poorly developed shatter cones near a very fractured quartz vein (Figures 10a and 10b).

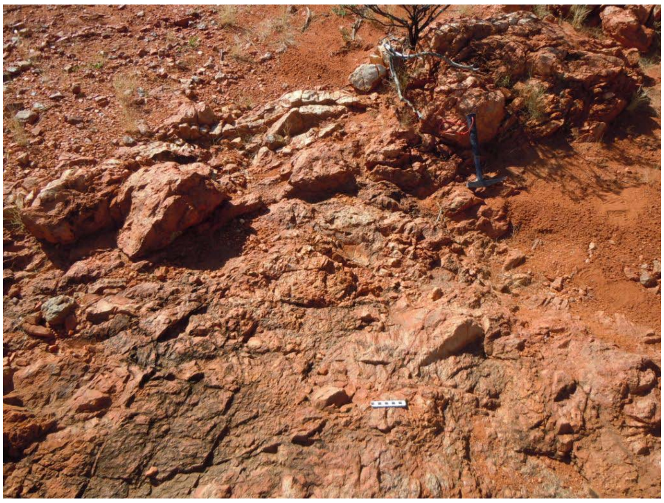

Figure 10a: Shattered granite at Locality 2. Scale: 10cm. Figure 10b: Detail of shattered granite at Locality 2.

Return south for 2.4 km, and just before the fence corner go through the gate. Turn north along the west side of the fence for 150m, turn left and go west for 600m. Turn right and follow the track north for 2.9 km to MGA 294100E 7141100N.

Locality 3: Leucocratic granite and quartz syenite of the Teague Granite

A traverse west for about 600 metres crosses patchy outcrop of Teague Granite. Much of it is leucocratic, but some has been defined as quartz syenite by Pirajno (2002). Much of the outcrop and subcrop is very fractured, and there are some poorly developed shatter cones. Quartz in thin section shows well developed PDFs (Figure 11). Pirajno's sample GSWA 152613 is located near here at MGA 29616E 7413460N. It is described as quartz-microcline-albite granite by Pirajno and albite–K-feldspar-quartz syenite by A. Y. Glikson (Appendix 2 in Pirajno, 2002), and was one of the samples that gave indeterminate Ar-Ar ages (D. Phillips, Appendix 3 in Pirajno, 2002).

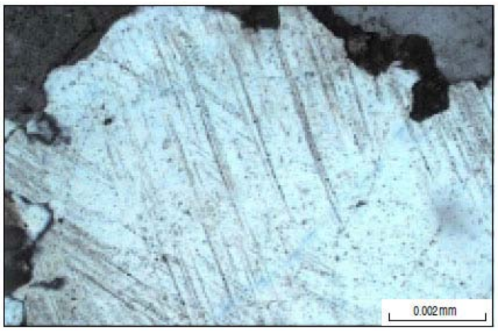

Figure 11: PDFs in quartz of Teague Granite. From Pirajno (2002).

Continue north along the track for 1.1 km to MGA 294100E 7142200N, turn left onto an old track and follow it west then southwest for 1.9 km to MGA 292460E 7141630N, about 200m north of the track.[Note that this locality was not visited during the preparation for this excursion, and there is no guarantee that access will be possible.]

Locality 4: Syenite of the Teague Granite

This is the site of sample GSWA 118996 from which Nelson (1997) obtained a SHRIMP U-Pb igneous crystallization age of 2648 +/- 8 Ma. Nelson described the rock as a pink, medium-grained equigranular syenite, composed of subequal amounts of microcline and albite with minor quartz (3-5%) and hornblende (2-3%). About 300m to the west at MGA 292150E 7141595 (coordinates from Pirajno, 2002) Johnson (1991) described one of several samples as aegirine-augite syenite.

Return 1.1 km to the north-south track and head north for 2.4 km to MGA 294100E 7144600N and turn left. Drive for about 200m.

Locality 5: Panorama view

With a very large structure and relatively low relief there is little opportunity to see the whole feature. From here

Figure 12: Panorama from near the centre of the Shoemaker impact structure, looking towards the rim. Note the line of hills (Frere Formation) and playa lakes.

there are views of much of the inner ring of hills of resistant Frere Formation, and the flat 12-km-diameter central uplift in more-easily eroded Archean rocks covered by playa lakes (Figure 12).

Continue west along the track for 1.8 km to MGA 292134E 7144740N.

Locality 6: Shatter cones in Frere Formation

South of the track outcrops of steeply dipping granular iron formation display some of the best shatter cones in the SIS (Figures 13 and 14). Some of the cones have large apical angles whereas others are more of the horsetail variety. Although secondary iron enrichment obscures some of the detail it is still possible to see the granular texture of the iron-formation, with rounded peloids of jasperoidal chert, generally 0.5-1.0 mm across, in a matrix of fine hematite and cryptocrystalline silica. Larger, more-tabular fragments, on a centimetre scale, are rip-up clasts (intraclasts). The peloids and intraclasts indicate a shallow-water environment above wave base. Elsewhere in the basin the granular iron-formation has an oolitic or pisolitic texture and, rarely, oncolites (large grains with concentric algal layering and abundant microfossils), indicating even shallower, shoal-like conditions. In the northern part of the Earaheedy Basin some banded iron-formations formed in deeper water.

If time permits the excursion will continue west along the track to investigate other outcrops of iron-formation with shatter cones, and examples of iron and manganese enrichment.

This then completes the Shoemaker part of the excursion. Retrace the track to the south, via Billabong Bore, to Millrose homestead and Wiluna.

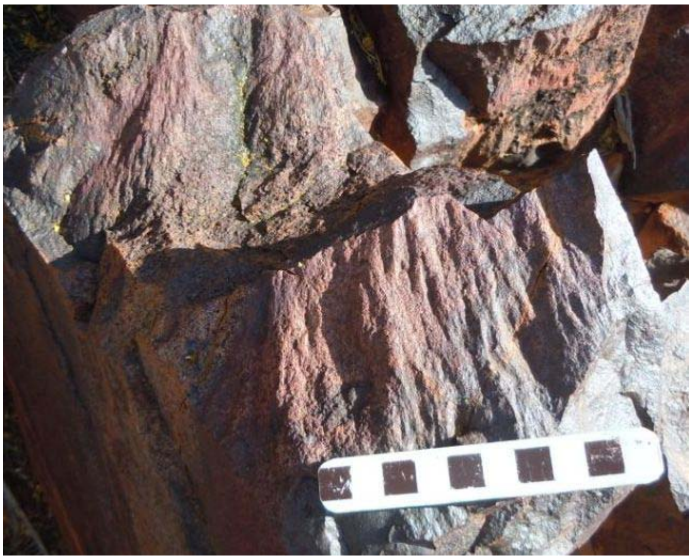

Figure 13: Horsetail structure on a shatter cone at locality 6. Scale is 10cm across.

Figure 14: Horsetail structure on a poorly-developed shatter cone in the Frere Formation. Scale is 10cm across.

References

Bunting, J. A., 1986. Geology of the eastern part of the Nabberu Basin. Geological Survey of Western Australia, Bulletin 131.

Bunting, J. A., Brakel, A. T. and Commander, D. P., Nabberu, W. A.,1980. Geological Survey of Western Australia, 1:250 000 Geological Series Explanatory Notes.

Bunting, J. A., De Laeter, J. R. and Libby W. G, 1980. Evidence for the age and cryptoexplosive origin of the Teague ring structure, Western Australia. Geological Survey of Western Australia, Annual Report 1979, p. 81-85.

Butler, H., 1974. The Lake Teague ring structure, Western Australia: an Astrobleme? Search, 5, p. 536-537.

Cassidy, C. F., Champion, D. C., Krapez, B., Barley, M. E., Brown, S. J. A., Blewett R. S., Groenewald, P. B. and Tyler, I. M., 2006. A revised geological framework for the Yilgarn Craton, Western Australia. Geological Survey of Western Australia, Record 2006/8, 8p.

Glikson, A.Y., 2002. Morphometric analysis and estimates of the original dimensions of the Shoemaker impact structure. In: Pirajno, F, 2002, Geology of the Shoemaker Impact Structure, Western Australia. Geological Survey of Western Australia Report 82.

Grey, K., 1984. Biostratigraphic studies of stromatolites from the Proterozoic Earaheedy Group, Nabberu Basin. Geological Survey of Western Australia, Bulletin 130.

Grey K., 1994, Stromatolites from the Palaeoproterozoic Earaheedy Group, Earaheedy Basin, Western Australia. Alcheringa, 18, p. 187-218.

Johnson, G. I., 1991. The petrology, geochemistry and geochronology of the felsic alkaline suite of the eastern Yilgarn Block, Western Australia. University of Western Australia PhD Thesis (unpublished).

Muhling, J. R., Fletcher, I. R. and Rasmussen, B., 2012. Dating fluid flow and Mississippi Valley type base-metal mineralization in the Paleoproterozoic Earaheedy Basin, Western Australia. Precambrian Research, 212-213, p. 75-90.

Nelson, D. R., 1997. Compilation of SHRIMP U-Pb zircon geochronology data, 1996. Geological Survey of Western Australia, Record 1997/2.

Nelson, D. R., 1999. Compilation of SHRIMP U-Pb zircon geochronology data, 1998: Geological Survey of Western Australia, Record 1999/2.

Pirajno, F., 1998. Nabberu, W. A. Sheet 3046. Geological Survey of Western Australia, 1:100 000 Geological Series.

Pirajno, F., 2002. Geology of the Shoemaker impact structure. Western Australia Geological Survey, Report 82.

Pirajno, F., 2005. Hydrothermal processes associated with meteorite impact structures: evidence from three Australian examples and implications for economic resources. Australian Journal of Earth Sciences, 52, p. 587-605.

Pirajno, F., and Glikson, A., 1998. Shoemaker Impact Structure Western Australia. Celestial Mechanics and Dynamical Astronomy, 69, p. 25-30.

Pirajno, F., Hawke, P., Glikson, A. Y., Haines, P. W., and Uysal, T., 2003. Shoemaker Impact Structure, Western Australia. Australian Journal of Earth Sciences, 50, p. 775-776.

Pirajno, F., Hocking, R. M., Reddy, S. M. and Jones, A. J., 2009. A review of the geology and geodynamic evolution of the Paleoproterozoic Earaheedy Basin, Western Australia. Earth Science Reviews, 94, p. 39-77.

Pirajno, F., Jones, J. A., and Hocking, R. M., 2004. Geology of the Nabberu and Granite Peak 1:100 000 Sheets. Western Australian Geological Survey 1:100 000 Geological Series.

Rasmussen, B., Fletcher, I. R., Bekker, A., Muhling, J. R., Gregory, C. J. and Thorne, A. M., 2012. Deposition of 1.88-billion-year-old iron formations as a consequence of rapid crustal growth. Nature, 484, p. 498-501.

Shoemaker, E. M. and Shoemaker, C. S., 1996. The Proterozoic impact record of Australia. Australian Geological Survey Organization, Journal of Australian Geology and Geophysics, 16, p. 2379-398.

Wingate, M. T. D., Pirajno, F. and Morris, P. A., 2004. Warakurna large igneous province,: a new Mesoproterozoic large igneous province in west-central Australia. Geology, 32, p. 105-108.

Notes

Figure 1: The "discovery" Google Earth image of the Hickman Crater. The crater is around 260m in diameter.

Hickman Crater

John Bunting

The Hickman Crater is 36 km north of Newman in the Pilbara region of Western Australia at 119°41'E 23°02'S. It was discovered in July 2007 by Arthur Hickman of the Geological Survey of Western Australia when he was using Google Earth. The circular nature of the feature, the flat floor and the raised rim hinted at a simple meteorite impact crater (Figure 1). Subsequent field and laboratory work by Andrew Glikson (Glikson et al., 2008) and, later, by Arthur Hickman (Hickman et al., 2008), found evidence to support an impact origin, including:

- fracturing and shattering of rhyolite and BIF;
- slickensides on blocks of rhyolite;
- radiating and plumose fractures;
- cryptocrystalline goethite veins with margins of altered rhyolite (hydrothermal alteration?);
- microfractures in quartz phenocrysts.

During a field visit to prepare for this excursion further evidence, possibly more diagnostic, for an impact origin was found, but this still needs confirmation by laboratory work.

Figure 2: Panorama of crater showing low hills of ejecta in SW (left-hand side). Note four-wheel drive vehicle for scale.

The Hickman Crater is in remote and hilly country high on the dissected plateau of the Ophthalmia Range. At the time of discovery (2007) there were no vehicular tracks near the crater (Figure 1). Current Google Earth imagery (October 2011) shows numerous tracks in and around the crater – the result of interest by Newman-based tour operators, independent visitors and mineral exploration companies, particularly Atlas Iron. Public access to the crater is via the Marble Bar road from Newman, then the road along the BHP Iron Ore railway and a track into the Poonda rock art site (Figure 3). Just before the rock art a track to the left heads southeast then west into the hills on a tortuous route to the crater. On this excursion we have permission from Atlas Iron to take a shorter route via the Atlas exploration camp (where we will camp for the night).

The following description of the crater is taken mainly from the work by Glikson et al. (2008) and Hickman et al. (2008 and PowerPoint presentation), plus the field visit by the organisers of this excursion, with regional geology from various GSWA publications.

Geological setting

The Hickman Crater straddles the contact between the Woongarra Rhyolite and the overlying Boolgeeda Iron Formation near the top of the early Paleoproterozoic Hamersley Group, on the southern flank of an east-southeast-plunging anticline (Figure 3). Beyond the influence of the crater dips are generally 15-25° to the south-southwest (Tyler, 1994).

The Woongarra Rhyolite is a regionally concordant giant lavalike felsic sheet, with an average thickness of 400 m and an area of at least 37 500 km^2 (Trendall, 1995). It has been subdivided into a lower unit, a median raft complex, and an upper unit. The rhyolite of the upper unit, with which we are dealing at Hickman, is commonly porphyritic and dark grey, with a subconchoidal fracture. Surface weathering has resulted in colours ranging from cream to buff and pinkish brown. In thin section phenocrysts of plagioclase and quartz (commonly resorbed) sit in a fine-grained, snowflake-textured matrix (Trendall, 1995).

Several features described by Trendall from the upper unit of the Woongarra Rhyolite could be important in understanding the Hickman Crater, in that they could be mistaken for impact-related effects, although none has been specifically identified. Autobrecciation is common near the top of the upper unit, with angular fragments commonly in the 10-100cm range. Flow layering is also present, although more common in the lower unit. Some plagioclase phenocrysts have coronas of micrographic intergrowths of quartz and feldspar. A feature of the contact with the overlying Boolgeeda Iron Formation is peperite, which is a mixture of fragmented magmatic and sedimentary material thought to have formed by intrusion of magma into wet sediment (Trendall, 1995). The intrusion of hot magma into the wet sediment caused vaporization of the water and explosive brecciation.

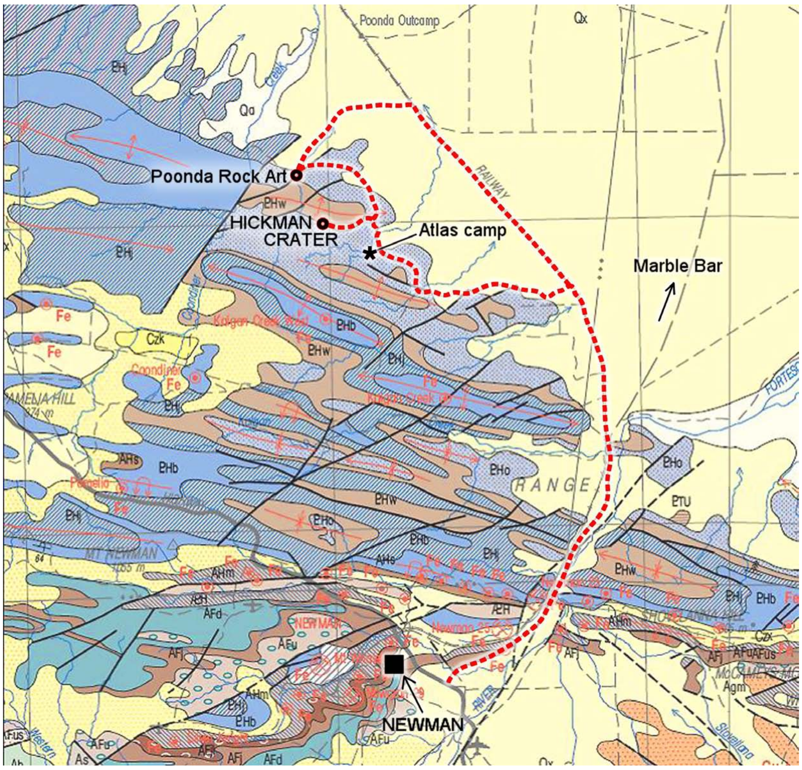

Figure 3: Regional geology, showing the position of Hickman Crater. PHb – Boolgeeda Iron Formation; PHw – Woongarra Rhyolite. Base map from GSWA Bulletin 144, Plate 1B.

The Boolgeeda Iron Formation consists of flaggy ironstone and iron-rich shale. The grey-black fine-grained ironstone, although loosely described as banded iron-formation (BIF), lacks the distinctive meso- and micro-banding of the BIF lower in the Hamersley Group (Weeli Wolli Formation, Brockman Iron Formation and Marra Mamba Iron Formation).

BIFs in the Pilbara contain some of the largest iron ore deposits in the world, principally in the Brockman and Marra Mamba Iron Formations and in channel and detrital iron deposits derived from them. Until recently the ironstones of the Boolgeeda Iron Formation were considered too low grade for mining, but the recent boom in the iron ore industry has seen a reappraisal of the Boolgeeda.

Metamorphism in the Hamersley Group is low-grade, reaching only lower greenschist facies. Open folds, on a regional and outcrop scale, have east-southeast axes, associated with weak axial surface cleavage and axial lineation. Gentle regional cross-folds have created a doubly plunging dome-and-basin pattern.

Crater Description

The Hickman Crater is almost circular (Figure 1), with a rim diameter of 250-270 m (average 260 m). The northern, eastern and southern rims, about 70% of the crater circumference, are uplifted 15-20 metres above the surrounding plateau surface and 20-30 m above the flat crater floor. The inner walls form steep, unstable slopes with numerous fallen blocks on the slopes and around the base (Figure 2 and Figure 4). Around the rim, bedding in the iron formation and crude flow layering in the rhyolites have been disrupted, steepened and in places overturned. Beyond the upturned rim,

Figure 4: Eastern wall and rim of the crater, with letter box.

Figure 5: Southwestern rim of the crater, with low ejecta-covered hills in the centre of the photograph. To the left is the "spillway", where the ejecta-blocked creek drains to the south.

angular fragments of rhyolite form an apron around the crater, with isolated fragments up to 300 m north of the crater. This is interpreted as part of an ejecta blanket.

The western/southwestern rim of the crater is lower and entirely covered with rhyolite and minor iron-formation ejecta (Figure 5). A pre-impact creek that enters the crater from the northwest would originally have flowed south, but it now terminates on the flat 170 m diameter crater floor. After heavy rain the floor of the crater must form a small lake. Alluvium deposited on the crater floor could be up to 20 m thick, and presumably overlies any impact-generated and fall-back breccia.

The exit point of the creek to the south has been blocked by an ejecta layer that now forms a lip about 3 m above the crater floor (Figure 5). This lip would be a spillway if the crater were to fill with water, with the overspill following a small creek that is eroding the ejecta downslope towards a major east-flowing creek.

Asymmetry of the crater

The ejecta-covered and topographically lower southwest portion, and distal ejecta up to 300m to the north, impart an asymmetry to the crater that prompted Glikson et al (2008) to suggest a south to north trajectory for the projectile, with a moderate angle of impact; however an abundance of rhyolite ejecta over Boolgeeda Iron Formation west-southwest of the crater may imply a west-southwest-directed impact (Hickman, pers. comm. in Glikson et al, 2008).

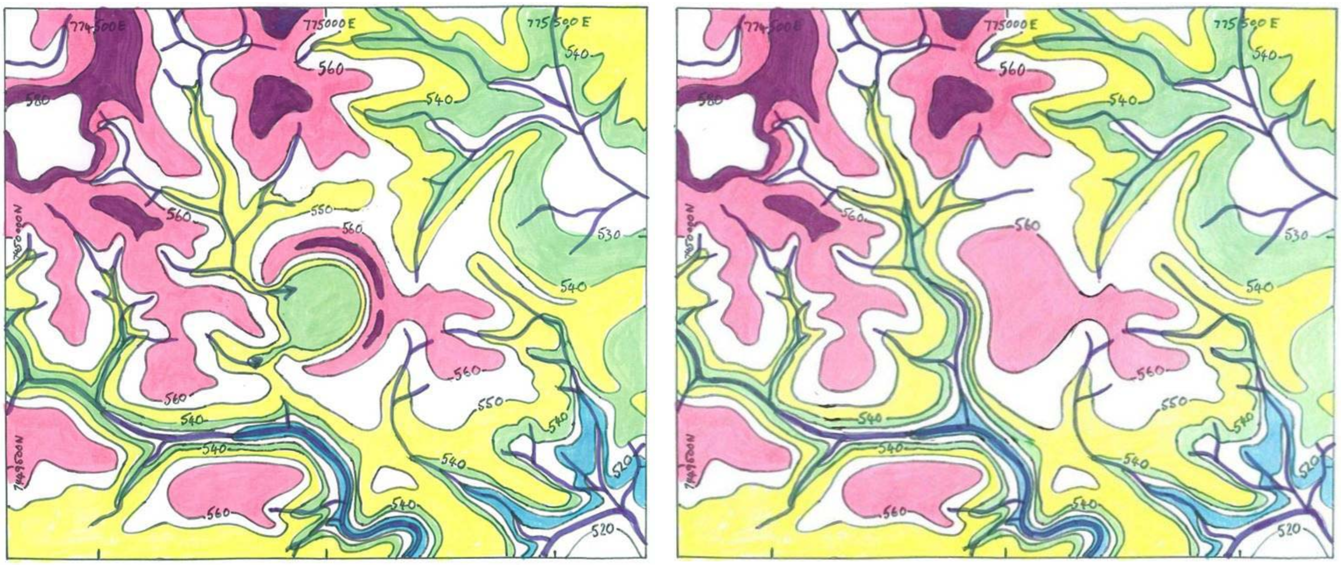

Figure 6: 6a – Present topography of the crater area; 6b – Reconstruction of topography prior to impact. Contours in metres above sea level. Field of view of each map is about 1400 metres. From Hickman et al. (2008) Powerpoint presentation.

On the basis of the preparatory field visit, the organisers of this excursion are of the opinion that the asymmetry is related to the pre-impact topography (Figure 6). Pre-impact the southeast- to south-flowing creek would almost certainly have flowed through a small gorge in the Woongarra Rhyolite and especially in the Boolgeeda Iron Formation. This is the typical situation for creeks of this size in this region. The impact, on the sloping plateau above and east of the creek, would have excavated a crater along an arc from northwest through east to south. Given that the point of impact was probably 30 m above the bed of the creek, and the base of the transient cavity was perhaps 30-40 m below the point of impact (on the basis of a 10 m iron projectile – Glikson et al., 2008), much of the energy of the impact would have dissipated sideways to the west and southwest, sending the ejecta into, across and down the creek rather than forming an upturned rim.

Age of the crater

The precise age of the impact is not known. Based on the drainage patterns and state of preservation of the rim impact may have been a few tens of thousand to possibly 100 000 years ago (Glikson et al., 2008). Preliminary isotope work on fracture surfaces indicates possibly 50 000 years as a good estimate (Hickman, pers. comm.). Research to refine this figure could include further isotope work on fracture surfaces, pollen analysis from a drillhole to the base of the crater-fill sediments, and carbon isotope analysis of any carbonaceous material.

Excursion localities

Warning: The steep inner rim of the crater is unstable and dangerous. We advise that you should not try to climb down from or up to the rim, but if you do, please accept the risk involved.

Because the excursion area is reasonably compact we are not going to suggest many specific localities, rather a general tour that could be modified depending on time and interests. We will park the cars near the southeast rim, where local tour operators have erected a letter box (Figure 4. MGA 775012E 7449717N) containing information about the crater and a visitors book.

There is a good view of the whole crater (Figure 2).

From the Letter Box walk northeast along the crater rim to view the upturned contact between the Boolgeeda Iron Formation and the Woongarra Rhyolite (MGA 775100E 7449780N).

The iron-formation is contorted and fractured. On the rhyolite look for shattered surfaces, slickensides, some of the goethite veining/nodules. From the eastern/northeastern rim you can walk downslope to see rhyolite blocks and fragments forming the ejecta blanket.

From the Letter Box, a walk down the slope, over rhyolite ejecta and BIF outcrop, takes you to the spillway (Figure 5). To the left (south) scramble down the slope into the small creek that is the post-impact rejuvenation of the pre-impact creek as it erodes through the ejecta layer.

The view to the south of the larger east-draining creek illustrates the low cliffs forming a gorge in Boolgeeda Iron Formation, typical of this region, which would be similar to that postulated for the north-south creek destroyed by the impact. BIF ejecta become more abundant as you descend the creek, and eventually the creek crosses BIF outcrop. Some of the BIF is weathered and brecciated (Figure 7a. MGA 774900E 7449630N), and 10 m further south boulders of BIF have slickensides and cross-cutting 2-3 mm veins that could be pseudotachylite (Figure 7b).

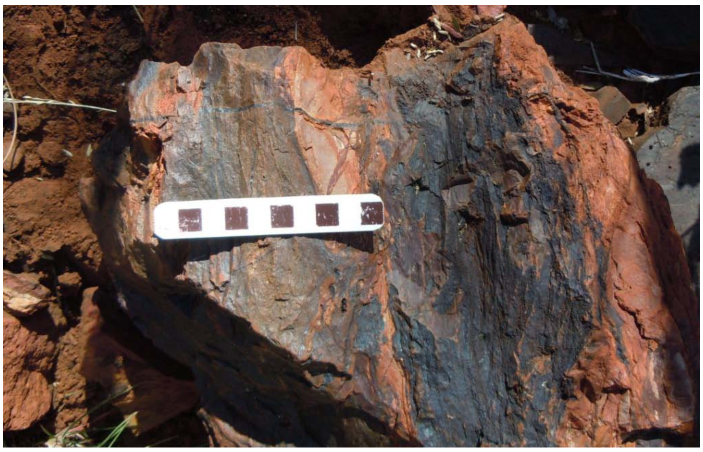

Figure 7: 7a – Brecciated BIF in rejuvenated creek below "spillway"; 7b – Boulder (ejecta?) of BIF with Fe-rich vein. Scale is in centimetres.

Returning to the spillway, walk into the crater and along its western side.

The low hills are entirely of rhyolite blocks, some of them car-size, that could be outcropping bedrock, but are more likely to be large masses of ejecta. In the hills further west, above a small creek, outcrop of flaggy BIF and ferruginous shale of the Boolgeeda is covered by ejecta fragments of both BIF and rhyolite. Look for pre-impact folds, cleavage and lineation. At MGA 273290E 7446600N fracture cleavage and lineation are well developed in thinly bedded (strike 300°/20° S) cherty, in part jaspilitic, BIF (Figure 8a, b). From here there is a good view north into the valley of the pre-impact creek system that drains southeast into the crater (Figure 9).

Figure 8: 8a – Outcrop of typical Boolgeeda Iron Formation; 8b – Fracture cleavage and lineation on cherty BIF. Scale is in centimetres.

Walk down the slope to the creek where it cuts the rim of the crater.

The creek here has cut a course between abutments of rhyolite, some of which may be outcropping upturned bedrock, but some is certainly blocks that have fallen down the slope. The narrow course of the creek has cut down into rhyolitic bedrock through about 1.5 m of crudely bedded pebbly alluvium.

On the northeast side of the creek at the bottom of the inner wall of the crater, look for a large block of rhyolite that has fallen from the crater wall (Figure 10a. MGA 774754E 7449687N). The block features numerous slickensides and complex fracturing. Note also the black iron-rich coatings, of unknown composition and origin but post-slickensides and perhaps related to post-impact weathering (Figure 10b).

Figure 9: View to NE from Figure 8a, showing SE-draining creek and, at right of picture, the abutment at the western end of the northern crater rim.

Figure 10: 10a – Fallen block of fractured rhyolite with slickensides; 10b – Detail from 10a, showing slickensides and black ferruginous coatings. Scale is 10 centimetres.

From here it is possible to walk back to the cars, either back along the creek, up the outside of the crater and east then south along the rim, or along the bottom of the inside eastern wall of the crater.

If taking the outside route, about 100 m north of the rim is Glikson's location H34 (Figures 2 and 7 in Glikson et al., 2008), at which you can see various veins and cavity fillings of iron-rich cryptocrystalline material in rhyolite.

References

Glikson, A. Y., Hickman, A. H. and Vickers, J., 2008, Hickman Crater, Ophthalmia Range, Western Australia: evidence supporting a meteorite impact origin: Australian Journal of Earth Sciences, 55, p 1107-1117.

Hickman, A. H., Glikson, A. Y. and Vickers, J., 2008, A newly discovered meteorite impact crater, Ophthalmia Range, Western Australia: Geological Society of Australia, Abstracts No. 89, p 133-134. (Also Powerpoint presentation, www.dmp.wa.gov.au/documents/Hickman_Crater.ppt).

Trendall, A. F., 1995, The Woongarra Rhyolite – a giant lavalike felsic sheet in the Hamersley Basin of Western Australia: Geological Survey of Western Australia, Report 42.

Tyler, I. M., 1994, Geology of the Newman 1:100 000 Sheet, Western Australia. Map Sheet SF50-16-2851, Explanatory Notes: Geological Survey of Western Australia.

Notes

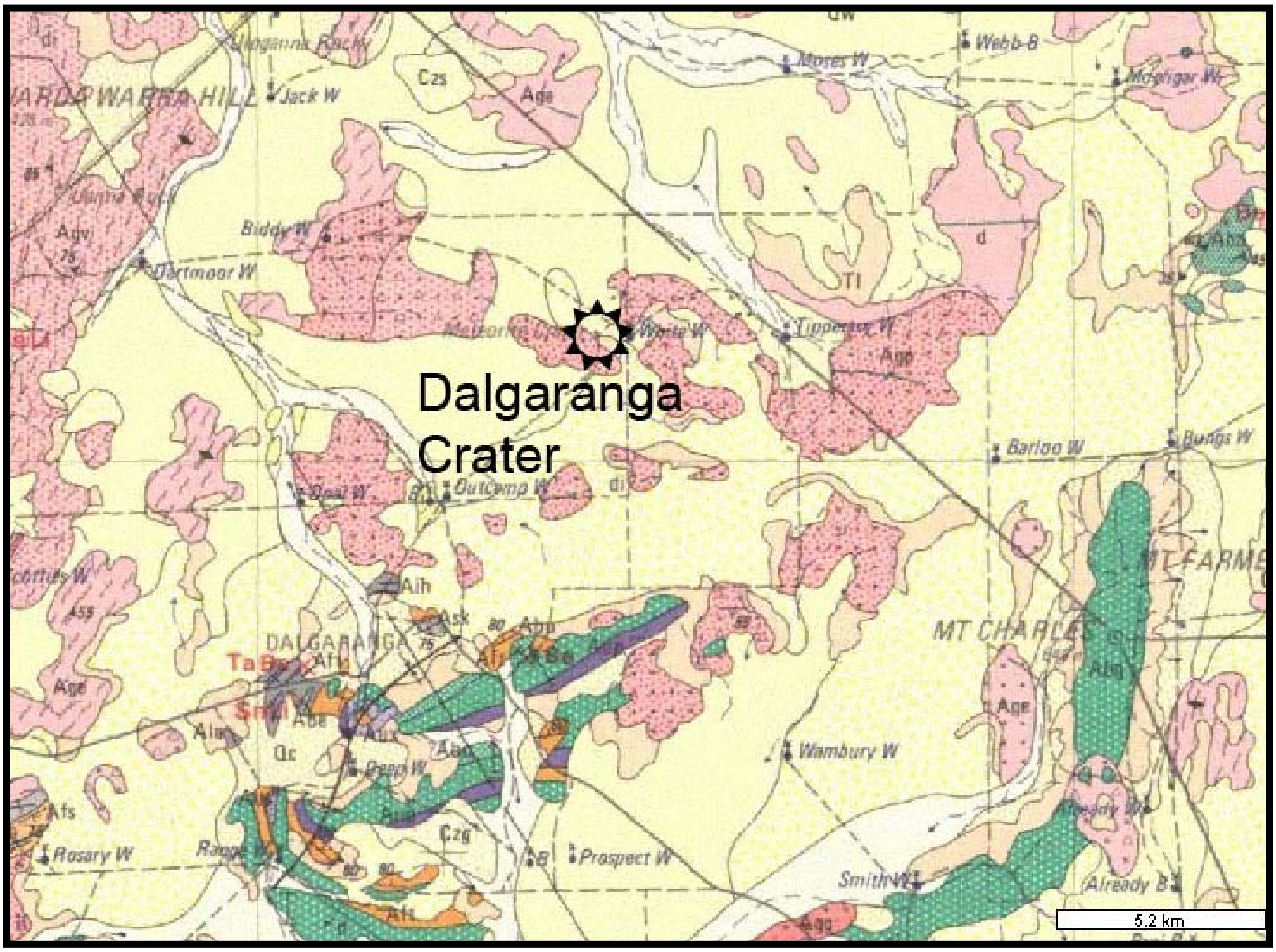

Figure 1: Geological setting of the Dalagaranga Crater. Age, Agp, Agv: biotite granites with granodiorite; Abg: gabbro; Af: felsic volcanics; Aup: peridotite; Tl: laterite.
Base map is from the Geological Survey of Western Australia 1:250 000 Geological Series: Cue, Sheet SG50-15.

Dalgaranga Meteorite Crater

Alex Bevan

Dalgaranga crater was reportedly first discovered by an aboriginal stockman in 1921 and later visited by G. E. P Wellard in 1923 who confirmed its meteoritic origin. Wellard collected fragments of the projectile (mesosiderite) but the whereabouts of the bulk of this material is unknown. The first mention in the scientific literature was not until 1938 based on the description of a single specimen (Simpson, 1938).

Figure 2: Dalgaranga crater.

Situated at 27˚ 39' 36.50"S 117˚ 17' 45"E, the crater is 24 m in diameter and approximately 3 m deep (Figure 2). In 1959 and 1960, additional collections of material were made by H. H. Nininger and G. I. Huss of the American Meteorite Laboratory. Two hundred and seven specimens totalling 1098 g were recovered from the area surrounding the crater, and 280 specimens totalling 9.1 kg were found beneath the crater floor (Nininger and Huss, 1960). Nininger and Huss excavated a pit located near the eastern edge of the crater floor.

Nininger and Huss (1960) and McCall (1965) showed that the impactor is a mesosiderite stony-iron. A modern analysis of the metallic portions of the meteorite by Wasson et al. (1974) gave 8.8% Ni, 15.5 ppm Ga, 56 ppm Ge, and 4.2 ppm Ir, confirming the mesosiderite classification. More recently, Hassanzadeh et al. (1990) re-analysed the meteorite which gave 10.27% Ni, 12.7 ppm Ga, and 4.99 ppm Ir, showing that the metallic portions of Dalgaranga vary in composition, particularly Ni. This is reflected in structural variations of the metallic portions of the meteorite which have Widmanstätten patterns that vary from finest to coarsest octahedrite.

Smith and Hodge (1996) reported abundant, weathered, microscopic meteorite particles in the soil around the crater. Much of the meteoritic material at Dalgaranga is corroded by prolonged terrestrial weathering. However, a substantial number of metal-rich slugs are well preserved. Structurally, the Widmanstätten patterns are variably deformed and locally show narrow (micrometre scale) zones of shear deformation along which metal has been recrystallised. This

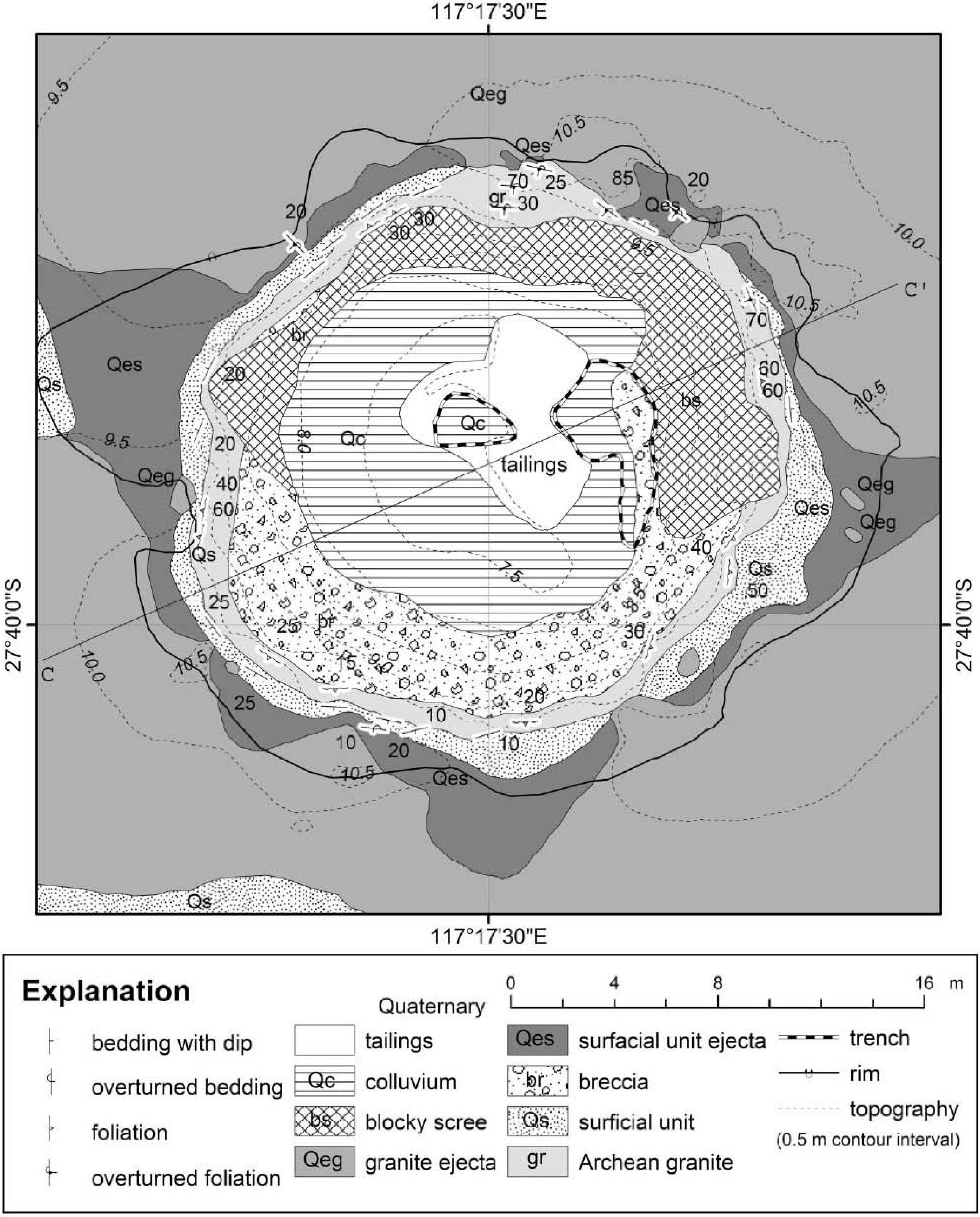

Figure 3: Geological map of Dalgaranga crater compiled by E. M. Shoemaker in 1986. Topographic contours are at 0.5 m intervals relative to an arbitrary base. (see Figure 6 for cross-section C-C'). From Shoemaker et al. (2005), copyright Australian Journal of Earth Sciences.

thermomechanical alteration is attributed to shock associated with impact and disruption (Bevan and Griffin, 1994; Bevan, 1996). Other fragments show little evidence of shock-metamorphism.

Dalgaranga was the first impact crater to be recognised in Australia and, with the exception of the small craters in the Henbury crater field, the smallest single crater in Australia. It is one of only two events known that were produced by a mesosiderite impactor (the other is Eltanin in the Bellinghausen Sea).

Setting and crater geology

Dalgaranga crater is situated in the Archaean granite-greenstone terrain of the Yilgarn Craton (Figure 1). The crater has been comprehensively described by Shoemaker et al. (2005) from which the following is a summary.

The crater walls are made of variably, and often severely, weathered granite (Figures 4 and 5). The granite, which is freshest on the southwest side of the crater, is a quartz-rich (up to 50%), medium grained granite. In the deeply weathered granite, feldspars have decomposed to clay minerals. On the eastern and northern sides of the crater the granite has been lateritised. In the most severely weathered cases, the granite has disintegrated to quartz sand with clay minerals.


Figure 4: Margin of Dalgaranga crater.

Outside the crater, the granite is overlain by a weakly stratified surficial unit of Quaternary age. This is a distinctive horizon (20-50 cm thick) that rests sharply on the granite and the contact allows definition the rim of the crater and hinge line. The unit is made principally of coarse-grained quartz set in a quartzite matrix consolidated by silica cement.

Impact lithologies and ejecta

In 1986, Gene and Caroline Shoemaker deepened Nininger's excavation to establish crater composition, accurate crater dimensions, and also to ensure that basement has been reached. The excavation penetrated about 0.5 m into the underlying impact breccia lens. The Shoemakers also made a detailed geological map (Figures 3 and 6). Within the crater, the breccia unit is well exposed around the southwest half and on the east wall in the excavation pit. The breccia consists mainly of fragmental weathered granite, but also contains fragments of the surficial unit and laterite. Clasts range in size from <1 cm to > 0.5 m. Exposures of the breccia on the southwest side of the crater are composed exclusively of granite clasts. Mixing of breccia lithologies occurs on the eastern side of the crater, notably in the excavation pit.


Figure 5: Large, tilted blocks on crater rim.

Mantling the lower part of the northern crater wall there is a chaotic blocky scree unit containing some large blocks. In contrast to the breccia lens, this talus unit is composed of loose material that appears to have slumped down from the crater wall. A contact between the scree and breccia lens below is exposed in the excavation pit. Above the talus there is 9.1m of post-impact colluvium, comprising small grains of quartzite and weathered granite fragments with occasional large blocks.

Surrounding the crater there are two ejecta units; ejecta from the surficial unit, and granite ejecta. The

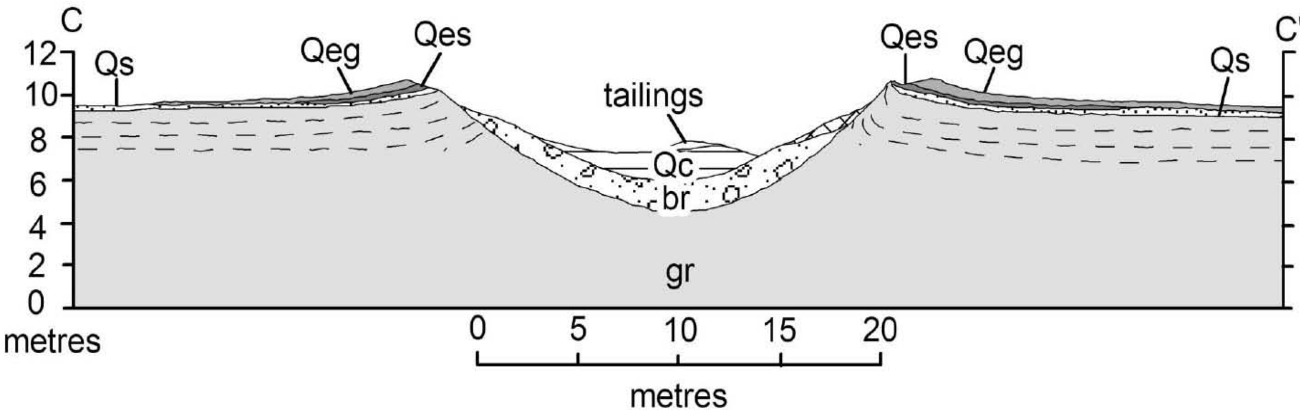

Figure 6: Geological cross-section of the Dalgaranga crater Elevations are relative to an arbitrary base. For unit identification see Figure 3. From Shoemaker et al. (2005), copyright Australian Journal of Earth Sciences.

surficial unit ejecta, underlies the granite ejecta and lies directly on the undisturbed Quaternary surficial unit. The granitic ejecta is largely chaotic. However, near the rim, some tabular granite ejecta blocks are clearly overturned (Figure 6) where some of the surficial unit remains attached. A few granite ejecta blocks measure more than a metre across, although most are <0.5 m. Large granite ejecta blocks are to be found on the northeast rim of the crater, some of which have been thrown more than 20 metres.

The distribution of ejecta around the crater, and a more complete overturning of rim and ejecta units on the northern side of the crater is consistent with an inferred direction of impact from the south-southwest. There is a pronounced bilateral symmetry in the ejecta units. There are two uprange ejecta rays at 60˚ from the inferred impact azimuth and 'forbidden' zones with little ejecta directly uprange and at 90˚ to the direction of impact (Figure 3). Shoemaker et al. (2005) note that this is a similar distribution to that produced in laboratory experiments by Gault and Wedekind, (1978) for an angle of impact between 10-15˚ from the horizontal.

Figure 6: Overturned blocks on crater rim.

Age

Clearly, from its state of preservation, Dalgaranga is a relatively 'young' crater. However, there is no consensus on the age of the crater. No glass has been recovered from the crater, placing limitations on age determination. Further, no attempt appears to have been made to determine a ^{14}C terrestrial age of the meteorite. A mean ^{10}Be-^{26}Al exposure age of 270 ka was obtained from granite bedrock near the crater rim from which a model erosion rate of $2x10^{-4}$ cm/yr was calculated for the surface at Dalgaranga. This is consistent with low erosion rates determined for other parts of the Australian landscape (Shoemaker et al., 1990). Other samples from breccia blocks gave relatively high ^{10}Be-^{26}Al abundances indicating pre-crater exposure and downward displacement of this material from near the original surface. However, all samples were expected to have exposure prior to cratering since the crater is very small.

However, the preservation of the subtle ejecta morphology led Shoemaker and Shoemaker (1988) to estimate that Dalgaranga crater was formed <3000 years ago. It is evident that impact occurred into an already partly weathered terrain.

Excursion Localities

There will be one stop: 27° 39' 36.50"S 117° 17' 45"E, to observe the features described in and around the crater (walking).

References

Bevan, A. W. R., 1996. Australian crater-forming meteorites. AGSO Journal of Australian Geology & Geophysics, 16(4):421-429.

Bevan, A. W. R. and Griffin, B. J., 1994. Re-examination of the Murchison Downs meteorite: a fragment of the Dalgaranga mesosiderite. Journal of the Royal Society of Western Australia, 77:45-49.

Gault, D. E. and Wedekind, J. A., 1978. Experimental studies of oblique impact. Proceedings of the 9th Lunar and Planetary Science Conference, pp.3843-3875.

Hassanzadeh, J., Rubin, A. E. and Wasson, J. T., 1990. Compositions of large metal nodules in mesosiderites: Links to iron meteorite group IIIAB and the origin of mesosiderite subgroups. Geochimica et Cosmochimica Acta 54:3197-3208.

McCall, G. J. H., 1965. New material from, and reconstruction of, the Dalgaranga meteorite and crater, Western Australia. Mineralogical Magazine 37:476-487.

Nininger, H. H. and Huss, G. I., 1960. The unique meteorite crater at Dalgaranga, Western Australia. Mineralogical Magazine 32:619.

Shoemaker, E. M., Macdonald, F. A. and Shoemaker, C. S., 2005. Geology of five small Australian impact craters. Australian Journal of Earth Sciences, 52:529-544.

Shoemaker, E. M. and Shoemaker, C. S., 1988. Impact structures of Australia. Lunar and Planetary Science Conference XIX (abstract).

Shoemaker, E. M., Shoemaker, C. S., Nishiizumi, K., Kohl, C. P., Arnold, J. R., Klein, J., Fink, D., Middleton, R., Kubik, P. W., and Sharma, P., 1990. Ages of Australian meteorite craters – A preliminary report. Meteoritics, 25:409.

Simpson, E. S., 1938. Some new and little-known meteorites found in Western Australia. Mineralogical Magazine 25:157-171.

Wasson, J .T., Schaudy, R., Bild, R. W. and Chou, C. L., 1974. Mesosiderites -I. Compositions of their metallic portions and possible relationship to other metal-rich meteorite groups. Geochimica et Cosmochimica Acta 38:135-149.

Smith, T. R. and Hodge, P. W., 1996. Microscopic meteoritic material at Dalgaranga, Odessa and Veevers meteorite craters. Lunar and Planetary Science Conference XXVII, 1223-1224.

Notes